The inertial migration of non-neutrally buoyant spherical particles in two-dimensional shear flows

By ANDREW J. HOGG

Institute of Theoretical Geophysics, Department of Applied Mathematics & Theoretical Physics, University of Cambridge, Silver Street, Cambridge CB3 9EW, UK

The inertial migration of a small rigid spherical particle, suspended in a fluid flowing between two plane boundaries, is investigated theoretically to find the effect on the lateral motion. The channel Reynolds number is of order unity and thus both boundary-induced and Oseen-like inertial migration effects are important. The particle Reynolds number is small but non-zero, and singular perturbation techniques are used to calculate the component of the migration velocity which is directed perpendicular to the boundaries of the channel. The particle is non-neutrally buoyant and thus its buoyancy-induced motion may be either parallel or perpendicular to the channel boundaries, depending on the channel alignment. When the buoyancy results in motion perpendicular to the channel boundaries, the inertial migration is a first-order correction to the magnitude of this lateral motion, which significantly increases near to the boundaries. When the buoyancy produces motion parallel with the channel boundaries, the inertial migration gives the zeroth-order lateral motion either towards or away from the boundaries. It is found that those particles which have a velocity exceeding the undisturbed shear flow will migrate towards the boundaries, whereas those with velocities less than the undisturbed flow migrate towards the channel centreline. This calculation is of practical importance for various chemical engineering devices in which particles must be filtered or separated. It is useful to calculate the forces on a particle moving near to a boundary, through a shear flow. This study may also explain certain migration effects of bubbles and crystals suspended in molten rock flow flowing through volcanic conduits.

1. Introduction

The migration of neutrally buoyant small particles across the streamlines of a laminar flow was first documented by Segré & Silberberg (1962a, b). Their study was motivated by the observation that blood corpuscles tend to be non-uniformly distributed across blood vessels. Segré & Silberberg performed experiments with dilute suspensions of rigid spheres in a laminar flow through a pipe, in the regime where the Reynolds number based on the pipe width was order unity or higher and found that the suspension developed a non-uniform concentration distribution over the pipe cross-section, which exhibited a peak concentration at a radial position of approximately 0.6 pipe radii. This result is thought to explain why the apparent viscosity of dilute suspensions in shear flows is lower than that predicted by Einstein's result (Segré & Silberberg 1962a, b; Ho & Leal 1974). The presence of particles increases the viscosity of the fluid and so the systematic cross-streamline migration implies that the velocity profile of the fluid across the pipe is flattened. Hence

calculations of an effective viscosity, based upon an assumption of a quadratic flow profile, will overpredict the actual viscosity of the suspension.

Following the work of Segré & Silberberg, there has been a series of experimental studies which consider the migration of particles with different properties, or migration within flows other than Poiseuille. Two investigations of particular relevance to this paper are the experimental studies of Jeffrey & Pearson (1965) and Eichhorn & Small (1964). These studies of non-neutrally buoyant particles within a vertical channel flow found that if the particle has a velocity greater than the undisturbed fluid velocity, then it migrates towards the channel boundaries, whereas if it lags behind the undisturbed fluid velocity, it migrates towards the channel centreline. In this paper, we investigate the migration of small non-neutrally buoyant spherical particles suspended in a fluid flowing between parallel plane boundaries. We calculate the migration velocity of the particles at varying positions across the channel and demonstrate agreement between the experimental results of Jeffrey & Pearson and the theoretical results computed here.

Bretherton (1962) showed that if inertia is neglected, no lateral force can exist for a body of revolution in a unidirectional flow. Hence the mechanism for cross-stream migration has been ascribed to the inertia of the fluid and particle and there have been a number of theoretical investigations of this effect. There are two ways by which the inertia of the fluid may influence the particle motion in a channel: inertial interaction with the wall, or, if the particle is moving in a sufficiently large domain, by the need to consider inertial effects in the far field. The latter is an expression of the need to include Oseen-like inertial corrections. Previous theoretical studies have focused on one or other of these effects, but have not studied the case in which both are significant. If we denote the channel Reynolds number by $R_c = U_m l/\nu$, where U_m is the channel centreline velocity, l is the channel width and ν is the kinematic viscosity, then the ratio of the magnitude of the wall effect to the Oseen-like inertial term is given by $R_c^{-\frac{1}{2}}$. This parameter may therefore be used to classify the previous studies, as discussed below and shown in table 1.

In the regime $R_c \ll 1$, the Oseen inertial correction is negligible in comparison with the inertial interaction with the walls. Within this regime, regular perturbation expansions based on small Reynolds number are permitted. Ho & Leal (1974) and Vasseur & Cox (1976) employed such expansions to predict the migration velocities for neutrally and non-neutrally buoyant particles moving within bounded fluid domains. Conversely, in the regime $R_c \gg 1$, the fluid may be treated as unbounded and the analysis need only consider Oseen-like regions. The formative study for this regime is that of Saffman (1965) who studied the lift force on a particle moving in a linear shear flow. Saffman showed that the lift force is of order $(R_p^{\frac{1}{2}})$, where R_p is the small particle Reynolds number based on the velocity gradient. Subsequent studies include those by Harper & Chang (1968), who studied the inertial lift and drag on a body with an arbitrary directed velocity, by Drew (1978), who included rotational flow, and by McLaughlin (1991), who accounted for the effect of uniform flow in the far field.

Other recent studies (Drew 1988; McLaughlin 1993; Shibata & Mei 1990) have considered the migration of a particle moving within a shear flow, bounded by a single rigid planar wall. These studies may not be classified by a channel Reynolds number because there is only one boundary. Sufficiently far away from this boundary, there is always an Oseen-like region in which viscous and inertial forces balance. Two of these studies (Drew 1988; McLaughlin 1993) assume that the boundary is sufficiently distant from the particle so that it lies within the region in which viscous and inertial forces balance. Drew (1988) assumed that the particle was moving parallel to the rigid planar wall, that the radius of the particle was much less than the distance to the wall and,

	Non-neutrally buoyant particles	Neutrally buoyant particles	Remarks
$R_c \ll 1$	Ho & Leal (1974) Vasseur & Cox (1976)	Ho & Leal (1974) Vasseur & Cox (1976)	Oseen-like inertial region is beyond the walls and so may use a regular perturbation expansion
$R_c = O(1)$	This study	Schonberg & Hinch (1989)	Wall effects and Oseen-like inertial region are significant
$R_c \gg 1$	Saffman (1965) Harper & Chang (1968) Drew (1978) McLaughlin (1991)	Lin, Perry & Schowalter (1970)	Wall effects are unimportant; Oseen-like inertial region only

TABLE 1. Classification of the theoretical studies of inertial migration, according to the channel Reynolds number. Each of the studies considers a small, rigid, spherical particle which is moving within a shear flow. Harper & Chang consider a body with an arbitrary directed velocity. Drew considers extentional and rotational flows. McLaughlin accounts for a uniform flow in the far field. (The author acknowledges the contribution of H. A. Stone to the compilation of this table. He suggested that the previous studies may be classified according to the channel Reynolds number and produced a version of this table.)

following the procedure of Saffman (1965), calculated the migration velocity of the particle. Drew's analysis, however, may not be applied to channel flow because a linear velocity profile was assumed which ignores the parabolic profile near to the channel centre. McLaughlin (1993) extended Drew's work by determining an algebraic expression for the migration velocity of a particle moving within a wall-bounded linear shear flow and by once again including uniform flow effects. The other study (Shibata & Mei 1990) assumes that the particle is moving sufficiently close to the boundary, so that the boundary lies within the region in which viscous forces dominate. The work of Shibata & Mei (1990) is motivated by considering the motion of sand particles within an oscillatory flow. However, the radius of the particle is assumed to be much smaller than the thickness of the Stokes boundary layer and hence the flow may be approximated by a linear shear flow, with a time-dependent rate of shear. Shibata & Mei (1990) calculate how the effect of including inertial forces in the far field, away from the boundary, influences the velocity field around the particle and hence the nature of particle interactions. This may have an important effect upon the way in which ripples form on a sandy bed under an oscillatory flow (Shibata & Mei 1990).

The parameter regime of order-unity channel Reynolds number is important because this is the regime in which experiments are typically performed. For example, Jeffrey & Pearson (1965) experimentally studied particle migration within a channel for $20 < R_c < 100$, while Segré & Silberberg (1962a, b) conducted their experiments at $2 < R_c < 700$. Furthermore, as indicated above, within this regime both wall effects and Oseen-like inertial effects are important. Schonberg & Hinch (1989) studied this regime for neutrally buoyant particles and the analysis developed in this paper is a generalization of their work to include non-neutrally buoyant particles. The theory uses a singular perturbation expansion within a 'far-field' region in which advective terms balance viscous terms. The particle is assumed to be sufficiently small to induce only a small disturbance to the background flow, thus allowing the linearization of the advective inertial term. A similar technique has been used by Vasseur & Cox (1977) to

study the migration of particles translating through stagnant fluid. Their calculation was also performed in the regime $R_c = O(1)$ and we shall show how their analysis may be reproduced within the theoretical framework presented here.

We present analyses for both vertically and horizontally aligned channels and calculate the lowest-order inertial correction to the cross-stream motion of the particle. As will be shown, this inertial correction to the cross-streamline motion of a non-neutrally buoyant particle is small in a horizontal channel. However, for a particle moving perpendicularly between planar boundaries, we find that by including only viscous forces and their interaction with the boundaries, the reduction of the velocity towards the boundaries can be significant. There have been a number of theoretical studies of a heavy spherical particle falling between plane boundaries, but analytical progress is difficult owing to the lack of a natural coordinate system in which both the no-slip conditions on the planes and sphere can be satisfied. Brenner (1961) used a bipolar coordinate system to select appropriate solutions to Laplace's equation and so derived an expression for the drag on a sphere as it approaches a single plane boundary. Ganatos, Weinbaum & Pfeffer (1980) used a 'boundary collocation' technique to study the problem of motion between an upper and lower boundary. Both of these studies are at zero Reynolds number, but it will be demonstrated that the results of Ganatos *et al.* (1980) may be reproduced under appropriate limits of the analysis presented in this paper.

In the next section of this paper, we present a derivation of the appropriate governing equations and boundary conditions for a sphere moving within a channel flow. These equations for the evolution of the disturbance flow, which is the disturbance caused by the introduction of the particle, are derived in a non-inertial frame of reference. Some care is necessary to derive the appropriate momentum equation in this frame, since the final result differs from that presented by Schonberg & Hinch (1989); in the limit they considered, though, the difference is negligible. Also we introduce three independent non-dimensional groups to characterize the problem. Two of these follow the definition of Schonberg & Hinch (1989), namely a lengthscale parameter and the channel Reynolds number, while the third expresses the ratio of the Stokes' settling velocity of the particle to the centreline velocity in the channel.

The solution via matched asymptotic expansions is outlined in §3. We construct an inner solution valid near the particle, derive appropriate governing equations valid in the outer region, where inertial effects are important and formulate the matching conditions. The equations are solved in §§4 and 5 and the migration velocities are calculated. Sections 4 and 5 correspond to different limiting regimes but the majority of the new analysis is contained within §4. The results are discussed in §6 and some comparison is made to experimental and other analytical studies. We also present straightforward physical arguments that account for the migration effects. Finally in §7, we present some applications of the calculations reported here. Appendices A–D present details of the calculation of the inertial migration, while Appendix E considers the inertial correction for the lift and drag on a sphere in an unbounded linear shear flow.

2. Formulation of the problem

2.1. *Governing equations*

We consider a parabolic flow profile between two infinite parallel planes separated by a distance l (figure 1). The steady flow is maintained by a constant pressure gradient acting parallel to the planes and the maximum flow velocity at the midpoint between
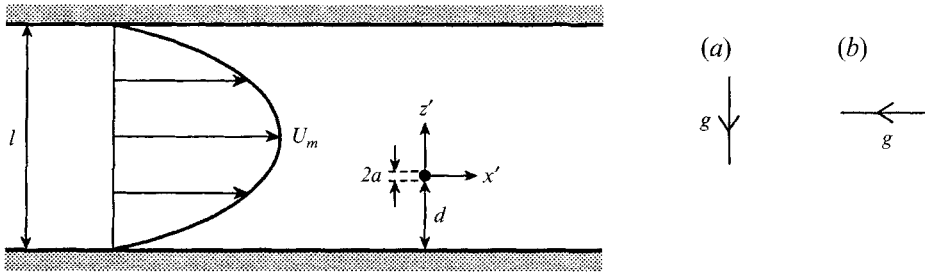
FIGURE 1. The configuration of the problem; characteristic lengths and velocities. (*a*) An horizontal channel, with gravitational acceleration perpendicular to the channel axis. (*b*) A vertically aligned channel, with gravitational acceleration parallel with the channel axis.

the planes is denoted by U_m. A spherical particle of radius a is moving in the flow at a position $Y(t)$. In principle, any shear flow could be analysed, but here Poiseuille flow is considered as the simplest flow that includes curvature in the velocity profile across the channel. Also, for simplicity, a two-dimensional geometry is considered but the calculation could be performed for a pipe of circular cross-section; such an extension of the analysis would produce more complex governing equations, but may be more appropriate for comparisons between theoretical and some experimental results.

The governing equations for the flow are the Navier–Stokes equation and the incompressibility condition,

$$\rho\left(\frac{\partial u}{\partial t}+u\cdot\nabla u\right)=-\nabla p+\mu\nabla^2 u, \tag{2.1a}$$

$$\nabla\cdot u=0. \tag{2.1b}$$

The flow in the absence of the particle, which we shall henceforth term the *undisturbed flow*, is given by

$$\bar{u}=\frac{4U_m}{l^2}z(l-z)\,\hat{x}, \tag{2.2}$$

where $\hat{x}$ is a unit vector aligned with the *x*-axis. There are three boundary conditions, representing a no-slip condition on the surface of the sphere (2.3*a*), a no-slip condition on the plane boundary (2.3*b*) and the absence of any disturbance to the flow away from the particle (2.3*c*):

$$u=U_p+\mathbf{\Omega}_p\wedge(x-Y)\quad\text{on}\quad|x-Y|=a, \tag{2.3a}$$

$$u=0\qquad\qquad\qquad\text{on}\quad z=0,l, \tag{2.3b}$$

$$u\rightarrow\bar{u}\qquad\qquad\qquad\text{as}\quad |(x-Y)\cdot\hat{x}|\rightarrow\infty, \tag{2.3c}$$

where U_p, $\mathbf{\Omega}_p$ are the linear and angular velocity of the particle. Denoting the Newtonian stress tensor by σ, the mass of the particle by m and the gravitational acceleration by g, the balance between the particle's drag, buoyancy and acceleration may be expressed as

$$\int_{|x-Y|=a}\sigma\cdot n\,\mathrm{d}S=-mg+m\frac{\mathrm{d}U_p}{\mathrm{d}t}. \tag{2.4}$$

We will demonstrate in §2.2 that within the regime of this study, the acceleration of the particle ($m\,\mathrm{d}U_p/\mathrm{d}t$) is smaller than either the drag on the particle or its buoyancy. Hence, for clarity, we ignore the acceleration term at this stage of the analysis. A series

of coordinate frame changes are made to ease the solution of the governing equations and imposed boundary conditions. First, the equations are transformed to a non-inertial frame of reference, in which the origin is instantaneously at the particle centre and moving with the particle velocity. We use a prime to denote variables in this moving frame and a dot to denote differentiation with respect to time. This change simplifies the no-slip boundary condition on the sphere (2.3a). The next change is to introduce the *disturbance flow*, defined as $w = u' - \bar{u}'$, which is the perturbation caused to the background undisturbed flow due to the introduction of the particle. Here the magnitude of the disturbance flow is expected to be small because the particle itself is small. We write the undisturbed flow $\bar{u}'$ in a frame moving with the sphere as

$$\bar{u}' \equiv \bar{u}^* - U_p^*, \tag{2.5}$$

where $\bar{u}^* = \bar{u} - \bar{u}(Y(t))$ is the undisturbed velocity in a frame moving with the undisturbed flow evaluated at the particle centre and $U_p^* = \dot{Y} - \bar{u}(Y(t))$ is the particle velocity in a frame moving with the undisturbed flow evaluated at the particle centre. The full governing equations and boundary conditions may then be written as

$$\rho \left(\frac{\partial w}{\partial t'} + w \cdot \nabla' w + \bar{u}^* \cdot \nabla' w - U_p^* \cdot \nabla' w + w \cdot \nabla' \bar{u}^* \right) = -\nabla'(p' - \bar{p}) + \mu \nabla'^2 w, \tag{2.6a}$$

$$\nabla' \cdot w = 0, \tag{2.6b}$$

$$w = U_p^* + \Omega_p \wedge x' - \bar{u}^*, \quad |x'| = a, \tag{2.6c}$$

$$w = 0, \qquad\qquad z' = -d, l - d, \tag{2.6d}$$

$$w \to 0, \qquad\qquad x' \to \pm \infty, \tag{2.6e}$$

$$\int_{|x'|=a} (\sigma(w) + \sigma(\bar{u})) \cdot n \, dS = -mg, \tag{2.6f}$$

where $\bar{u}^* = 4U_m[(1 - 2d/l) z'/l - z'^2/l^2] \hat{x}$ and the distance of the particle from the wall is given by $d = Y \cdot \hat{z}$.

2.2. *Non-dimensionalization*

The problem can be characterized by three independent non-dimensional groups: the lengthscale parameter, $\alpha = a/l$, which is the ratio of particle to channel lengthscales; the channel Reynolds number, $R_c = U_m l/\nu$, which is the ratio of inertial to viscous forces for the channel; and a buoyancy number, $B = \frac{2}{9} a^2 \Delta \rho g / \mu U_m$, which is the ratio of the Stokes' settling velocity to the channel centreline velocity. In addition, the parameter $R_p = U_m a^2 / \nu l = \alpha^2 R_c$ will be used, which is the particle Reynolds number based upon the particle radius and average velocity gradient. These parameters follow the definitions of Schonberg & Hinch (1989) and express the importance of the particle's size, inertia and buoyancy. Other studies (e.g. Vasseur & Cox 1976; Jeffrey & Pearson 1965) have chosen a different set of independent parameters, but they can all be expressed in terms of the ones defined above.

The governing equations are now non-dimensionalized by the particle lengthscale a and the Poiseuille flow velocity U_m. We continue to work in a frame moving with the velocity of the centre of the sphere, but for clarity the prime notation is dropped and the variables are now considered to be dimensionless variables. The equations are therefore

$$\frac{R_p}{\alpha} \left(\frac{\partial w}{\partial t} + w \cdot \nabla w + \bar{u}^* \cdot \nabla w - U_p^* \cdot \nabla w + w \cdot \nabla \bar{u}^* \right) = -\nabla p + \nabla^2 w, \tag{2.7a}$$

$$\nabla \cdot w = 0, \tag{2.7b}$$

and the boundary conditions are given by

$$w = U_p^* + \Omega_p \wedge x - \bar{u}^*, \quad |x| = 1, \tag{2.8a}$$

$$w \to 0, \qquad\qquad x \to \pm\infty, \tag{2.8b}$$

$$w = 0, \qquad\qquad z = -d/l\alpha, \quad (1-d/l)/\alpha, \tag{2.8c}$$

$$\int_{|x|=1} (\sigma(w) + \sigma(\bar{u})) \cdot \hat{n} \, \mathrm{d}S = -6\pi B \hat{g}, \tag{2.8d}$$

where $\bar{u}^* = (\alpha\gamma z - 4\alpha^2 z^2)\hat{x}$, $\gamma = 4 - 8d/l$ is the shear rate, non-dimensionalized with respect to U_m and l, and $\hat{g}$ is a unit vector in the direction of the gravitational force. This analysis is based upon the regime of small particles compared to the channel width, which implies $\alpha \ll 1$, the channel Reynolds number of order unity, $R_c = O(1)$ (or higher, subject to the constraints that the flow must be laminar which limits the channel Reynolds number to less than approximately 2000) and arbitrary values of the buoyancy number. We consider cases ranging from one in which the sedimentation of the particle dominates the flow field through to the case of a neutrally buoyant particle.

At this stage we introduce some typical dimensional lengthscales for the problem which justify the claim of §1 that this parameter regime includes both Oseen and wall inertial effects and which describe some of the parameter ratios relevant to the asymptotic analyses of §§3–5. The lengthscale at which inertial effects are important, based on the centreline velocity, is given by

$$l_{U_m} = \nu/U_m = l/R_c. \tag{2.9}$$

The inertial lengthscale, based on a typical shear rate for the channel flow, is

$$l_{shear} = (\nu l/U_m)^{\frac{1}{2}} = l/R_c^{\frac{1}{2}}. \tag{2.10}$$

The inertial lengthscale, based on particle sedimentation, is

$$l_{sed} = \nu/u_{settling} = l/BR_c. \tag{2.11}$$

Both l_{U_m}/l and l_{shear}/l express the ratios of the distance from the particle at which inertial effects are important relative to the width of the channel. From (2.9) and (2.10), we note that if $R_c = O(1)$, all these lengthscales (l_{U_m}, l_{shear}, l) are comparable. Therefore we find that there are fluid regions in which inertia is important within the channel, which introduces Oseen-like inertial corrections in addition to those arising from irreversible inertial interaction with the boundaries. The ratio $l_{shear}/l_{sed} = BR_c^{\frac{1}{2}}$ is the ratio of the distances from the particle at which inertial effects arising from the shear flow in the channel and from particle sedimentation, become important. The magnitude of this ratio determines whether the inertial corrections are dominated by sedimentation or by shear effects.

We also assess the magnitude of the acceleration of the particle and justify neglecting it, when balancing the forces on the particle (2.4), (2.6f), (2.8d). The timescale over which the particle accelerates in response to moving through the mean flow is given in dimensional form by $\tau \sim l/U_p$. Hence the magnitude of the ratio of the acceleration of the particle to the viscous stress acting on it is given by

$$O\left(m\frac{\mathrm{d}U_p}{\mathrm{d}t} \middle/ \int \sigma \cdot \hat{n} \, \mathrm{d}S\right) = \frac{\rho + \Delta\rho}{\rho} \alpha^2 B^2 R_c. \tag{2.12}$$

Hence to justify neglecting the acceleration of the particle, we require

$$\alpha^2 B^2 R_c \ll 1. \tag{2.13}$$

For the regime studied here, this is not restrictive since $\alpha \ll 1$ and $R_c = O(1)$. The condition solely excludes a steady-state analysis of the motion of particles, whose Stokes settling velocities greatly exceed the undisturbed velocity along the centreline of the channel.

3. Solution via matched asymptotic expansions

The problem is solved using the method of matched asymptotic expansions. An 'inner' Stokesian layer is constructed around the sphere, which satisfies the no-slip boundary condition on it. This approximate solution is matched to an 'outer layer' in which viscous forces are balanced by the advective inertia terms and the boundary conditions are satisfied at the channel edges.

3.1. *Inner problem*

In the limit $R_p/\alpha \ll 1$ we propose an inner expansion for the disturbance flow and pressure fields in ascending powers of this parameter ratio,

$$w = w_0 + O(R_p/\alpha), \quad p = p_0 + O(R_p/\alpha). \tag{3.1}$$

This yields the following 'creeping flow' equations and boundary conditions for the sphere:

$$\nabla^2 w_0 - \nabla p = 0, \tag{3.2a}$$

$$\nabla \cdot w_0 = 0, \tag{3.2b}$$

$$w_0 = U_p^* + \Omega_p \wedge x - (\alpha\gamma z - 4\alpha^2 z^2)\,\hat{x}, \quad r = 1, \tag{3.2c}$$

$$w_0 \to 0, \qquad\qquad\qquad r \to \infty. \tag{3.2d}$$

These equations may be solved using spherical harmonics (Lamb 1932). Since the equations are linear, we construct solutions which correspond to each of the boundary conditions on the sphere.

(i) The solution driven by the boundary condition $w_0 = U_p^*$ on $r = 1$ is

$$w_0 = U_p^* \left(\frac{1}{4r^3} + \frac{3}{4r} \right) + x \frac{U_p^* \cdot x}{r^2} \left(-\frac{3}{4r^3} + \frac{3}{4r} \right). \tag{3.3}$$

This solution gives no couple and a drag force of $-6\pi U_p^*$ on the sphere.

(ii) The solution driven by the boundary condition $w_0 = \Omega_p \wedge x - \alpha\gamma z\hat{x}$ on $r = 1$ is

$$w_0 = (\Omega_p - \omega) \wedge x \frac{1}{r^3} - E \cdot x \frac{1}{r^5} - x \frac{5 x \cdot E \cdot x}{2} \frac{1}{r^2} \left(\frac{1}{r^3} - \frac{1}{r^5} \right), \tag{3.4}$$

where
$$E = \begin{pmatrix} 0 & 0 & \frac{1}{2}\alpha\gamma \\ 0 & 0 & 0 \\ \frac{1}{2}\alpha\gamma & 0 & 0 \end{pmatrix} \quad \text{and} \quad \omega = \begin{pmatrix} 0 \\ -\frac{1}{2}\alpha\gamma \\ 0 \end{pmatrix}.$$

This solution gives no drag force and a couple of $8\pi(\Omega_p - \omega)$ on the sphere. Hence, since the particle is torque-free, the particle angular velocity is equal to half the local shear rate (i.e. $\Omega_p = \omega$).

(iii) The solution driven by the boundary condition $w_0 = 4\alpha^2 z^2 \hat{x}$ on $r = 1$, corresponding to the parabolic part of the undisturbed flow, is derived in Appendix A. Written in terms of spherical polar coordinates (r, θ, ϕ), with the $\theta = 0$ axis aligned along the x-axis, the disturbance velocity is given by

$$\frac{w_{0r}}{\alpha^2} = \cos\theta \sin^2\theta \cos 2\phi \left(-\frac{5}{r^5} + \frac{7}{r^3} \right) + \cos^3\theta \left(\frac{5}{r^5} - \frac{7}{r^3} \right) + \cos\theta \left(-\frac{3}{r^5} + \frac{3}{r^3} + \frac{2}{r} \right), \quad (3.5a)$$

$$\frac{w_{0\theta}}{\alpha^2} = \sin^3\theta \cos 2\phi \left(-\frac{15}{4r^5} + \frac{7}{4r^3} \right) + \sin\theta \cos 2\phi \left(\frac{5}{2r^5} - \frac{5}{2r^3} \right)$$

$$+ \sin^3\theta \left(-\frac{15}{4r^5} + \frac{7}{4r^3} \right) + \sin\theta \left(-\frac{1}{r} - \frac{2}{r^3} + \frac{3}{r^5} \right), \quad (3.5b)$$

$$\frac{w_{0\phi}}{\alpha^2} = \sin\theta \cos\theta \sin 2\phi \left(-\frac{5}{2r^5} + \frac{5}{2r^3} \right). \quad (3.5c)$$

This solution gives no couple and a drag force of $-8\pi\alpha^2 \hat{x}$ on the sphere.

These components of the solution are combined to give the complete form of the first term in the inner expansion (w_0). We may apply the force balance to give the particle velocity, measured in a frame of reference moving with the undisturbed velocity at the particle centre. This gives

$$U_p^* = B\hat{g} - \tfrac{4}{3}\alpha^2 \hat{x}. \quad (3.6)$$

We note that the magnitude of the buoyancy and the orientation of the channel determine the motion perpendicular to the undisturbed-flow streamlines according to this zero-order solution in the inner layer. A neutrally buoyant particle $(B = 0)$, therefore, exhibits no lateral migration at this order of solution, nor does a particle in a channel aligned with the gravitational acceleration. The term arising from the parabolic flow profile across the channel $(-\tfrac{4}{3}\alpha^2 \hat{x})$ indicates that the particle lags the undisturbed flow. This lag results from a particle drop across the particle and is expressed by the spherical harmonic p_{-2}^0 of the pressure field (Appendix A).

For matching to the outer layer we examine the far-field behaviour of this Stokesian solution. As $r \to \infty$, the disturbance flow field takes the form

$$w_0 = \underbrace{U_p^* \frac{3}{4r} + x \frac{U_p^* \cdot x}{r^2} \frac{3}{4r}}_{O(B/r)} - \underbrace{x \frac{5}{2} \frac{x \cdot E \cdot x}{r^5}}_{O(\alpha\gamma/r^2)} + \underbrace{\hat{x} \frac{\alpha^2}{r} + x \frac{\alpha^2 x}{r^3}}_{O(\alpha^2/r)} + O\left(\frac{1}{r^3}\right). \quad (3.7)$$

Using the results and definitions of Appendix B, we may interpret each of these far-field terms. The first term, which is $O(B/r)$, is a 'Stokeslet' due to particle migration and is only non-zero for a non-neutrally buoyant particle. The second, which is $O(\alpha\gamma/r^2)$, is a 'strainlet' due to the linear shear on the particle. The third, which is $O(\alpha^2/r)$, is a 'Stokeslet' due to the quadratic profile of the undisturbed flow.

For the matching procedure, we need to establish which of these conditions is dominant in the far field at the plane boundaries. This determination depends on the relative magnitude of the parameters B and α, since even though the strainlet terms decays more rapidly than the Stokeslet, it is still feasible that it dominates if the local shear rate $(\alpha\gamma)$ greatly exceeds the buoyancy. In non-dimensional terms, the plane boundary occurs at $r \sim 1/\alpha$ and so, away from the channel centreline, the Stokeslet

term arising from the quadratic profile of the undisturbed flow can never dominate the strainlet term, due to the linear shear on the particle. Hence, we have the following far-field behaviour:

(i) if $B > \alpha$, then the Stokeslet term $O(B/r)$ dominates throughout;

(ii) if $B < \alpha$, then $\begin{cases} \text{strainlet } O(\alpha\gamma/r^2) \text{ dominates for } 1 \ll r \ll \alpha/B, \\ \text{Stokeslet } O(B/r) \text{ dominates for } \alpha/B \ll r. \end{cases}$

The dominant term at the plane boundaries determines the form of the outer layer. Hence, we must consider which term dominates at distances $r \sim 1/\alpha$ and, according to (3.7), this is established by the value of the ratio α^2/B compared with unity.

It is possible to make a regular perturbation calculation of the next term in the inner expansion. This term is formally of $O(R_p/\alpha)$ and details of the calculation are given in Appendix C. However, as will be demonstrated, it is not necessary to calculate it to achieve first-order matching.

3.2. *Outer problem*

The Stokesian layer around the sphere describes a short-range solution, which decays like $O(1/r)$. At greater distances from the sphere it is necessary to consider a region in which the viscous forces are balanced by the advective terms. This is similar to the problem of a sphere translating through an unbounded fluid, which exhibits Whitehead's paradox. It is not possible to find a regular perturbation correction to the Navier–Stokes equations, for small but non-zero Reynolds numbers, that is consistent at all distances from the sphere. The inertial terms involve a first-order spatial derivative, whereas the viscous terms involve a second-order derivative. Thus if the velocity field decays as r^{-n}, it is inevitable that at sufficiently large distances the two forces are comparable. Oseen's improvement to the procedure for calculating the approximate solution to the equations of motion was to decompose the fluid velocity into a component moving with the sphere's velocity and a component representing the disturbance to the background flow. On the assumption that the sphere induces little disturbance to the flow, the acceleration terms of the equation may then be linearized. (Using the notation developed here, this is equivalent to neglecting the term $\mathbf{w} \cdot \nabla \mathbf{w}$.) This approximation is uniformly valid throughout the flow domain, provided $R_p/\alpha \ll 1$, as pointed out by Batchelor (1965).

We construct an outer region, distant from the particle, within which viscous and inertial forces are comparable. We introduce an outer spatial coordinate, linked to the inner one via some linear scaling,

$$X = Sx, \tag{3.8}$$

and we denote the velocity and pressure fields in the outer region by $W(X) = w(x)$, $P(X) = p(x)$.

In order to determine the first term of the outer-region expansion, it is necessary to match the outer solution $W(X)$ as $X \to 0$ to the inner solution $w_0(x)$ as $|x| \to \infty$. This matching ensures that the solutions arising from the Stokes region and from the outer region, where viscous and inertial forces are comparable, agree in some 'overlap domain'. This matching procedure is elementary for this problem and could be carried out using Van Dyke's matching rule or using an intermediate-variable technique (Hinch 1992). However, following the approach of Saffman (1965), we encapsulate the matching conditions into the momentum equation by the introduction of a suitable forcing term. Saffman represented a general forcing by a Taylor series involving successive derivatives of the delta function and demonstrated that for the expansion to lowest order in the outer region it is necessary only to utilize the dominant term of this Taylor expansion. Hence, noting the calculations of Appendix B and noting the

behaviour of the inner solution as $r \to \infty$ (see §3.1), we introduce the point forcings into the momentum equation as a means of matching the first-order inner and outer fields. Denoting $R = |X|$, we find that the Stokeslet and strainlet velocity fields may be replaced by a delta function and a linear combination of derivatives of the delta function, respectively. Thus we replace

$$W \to S(3/4R)(U_p^* + (U_p^* \cdot X/R^2) X) \quad \text{as} \quad R \to 0 \quad \text{with} \quad 6\pi S^3 U_p^* \delta(X), \quad (3.9\,a)$$

$$\text{and} \quad W \to -5S^2/2(X \cdot E \cdot X/R^5) X \quad \text{as} \quad R \to 0 \quad \text{with} \quad -\tfrac{20}{3}\pi S^4 E \cdot \nabla \delta(X). \quad (3.9\,b)$$

Hence we find that the governing equation in the outer region is given by

$$\frac{R_p}{\alpha}\left(\frac{\partial W}{\partial t} + SW \cdot \nabla W + \underbrace{S\bar{U}^* \cdot \nabla W + SW \cdot \nabla \bar{U}^*}_{\text{inertia 1}} - \underbrace{SU_p^* \cdot \nabla W}_{\text{inertia 2}}\right) = -S\nabla P + \underbrace{S^2 \nabla^2 W}_{\text{viscous}}$$

$$+ \begin{cases} 6\pi S^3 U_p^* \delta(X), & \alpha^2/B \ll 1, \\ -\tfrac{20}{3}\pi S^4 E \cdot \nabla \delta(X), & \alpha^2/B \gg 1, \end{cases} \quad (3.10)$$

where $\bar{U}^* = (\alpha\gamma Z - 4\alpha^2 Z^2)\hat{X}$. We argue below that the dominant balance in this equation is between the inertial terms, denoted inertia 1 and 2, and the viscous term. The flow is driven by the point forcing, which represents the matching of the inner to the outer solution and which determines the scaling of the leading-order outer flow velocity. The terms denoted inertia 1 arise from the inertia of the shear flow in the outer region, whereas the term denoted inertia 2 arises from the inertia of the flow field associated with the motion of the particle. In the far field we balance the viscous terms with one of the inertial terms and this provides the scaling of the outer region (3.8).

We make an Oseen-like approximation and linearize the acceleration terms in this governing equation, as discussed above. Here this neglects the term $W \cdot \nabla W$ and implies that the wake around the particle does not interact with itself. This approximation is justified since in the far field $O(W \cdot \nabla W) \ll O(\bar{U}^* \cdot \nabla W + W \cdot \nabla \bar{U}^*)$, $O(U_p^* \cdot \nabla W)$. The magnitude of the time-derivative term may be assessed by a simple scaling argument. If we neglect the time variation of the disturbance flow ($T_f \sim l^2/\nu$), then the flow must be established much faster than the time over which the particle moves towards the boundaries $T_b \sim l/u_{lateral}$. This condition requires

$$T_f/T_b \sim R_c u_{lateral}/U_m \ll 1. \quad (3.11)$$

This condition is satisfied in a vertically aligned channel since the lateral migration velocity is small. However, with a horizontally orientated channel, the lateral migration velocity scales with the Stokes' settling velocity of the particle. Hence we require

$$T_f/T_b \sim BR_c \ll 1 \quad (3.12)$$

for the quasi-steady solution to be valid. If the condition (3.12) is not satisfied, the time variation of the velocity may not be neglected because the time taken for a particle to translate towards the boundary is less than the time taken to establish the flow field. In this paper, we focus on solving only the steady-state equations and so (3.12) must be satisfied for a horizontally aligned channel.

Substituting the undisturbed flow field in terms of the outer coordinate into (3.10) and balancing the viscous and inertial terms, we find that there are two possibilities for the outer-region scaling:

  (i) viscous terms balance advective terms due to undisturbed shear velocity,

$$S = R_p^{\frac{1}{2}} \quad \text{if} \quad 1 \gg B^2 R_c; \quad (3.13\,a)$$

(ii) viscous terms balance advective terms due to sphere migration,

$$S = R_p B/\alpha \quad \text{if} \quad 1 \ll B^2 R_c. \tag{3.13b}$$

This product of parameters, $B^2 R_c$, was established in §2.2. Essentially its magnitude represents which of the inertial contributions dominates. Previous investigators (e.g. Saffman 1965, McLaughlin 1991) have expressed this product as the ratio of the square of the particle Reynolds number based on slip velocity to the particle Reynolds number based on velocity gradient. We now pose outer expansions for the pressure and velocity fields,

$$W(X) = W_0(X) + O(R_p/\alpha), \quad P(X) = SP_0(X) + O(R_p/\alpha). \tag{3.14}$$

Therefore the governing equations for this first term in the outer expansion, after linearizing, neglecting the time derivatives and including the matching condition to the inner solution by means of a point forcing, are

$$\nabla^2 W_0 - \nabla P_0 + \begin{cases} 6\pi S U_p^* \,\delta(X) & (\alpha^2/B \ll 1) \\ -\frac{20}{3}\pi S^2 E \cdot \nabla\delta(X) \,(\alpha^2/B \gg 1) \end{cases} = \begin{cases} \bar{U}^* \cdot \nabla W_0 + W_0 \cdot \nabla \bar{U}^* & (1 \gg R_c B^2) \\ -U_p^* \cdot \nabla W_0 & (1 \ll R_c B^2), \end{cases} \tag{3.15a}$$

$$\nabla \cdot W_0 = 0, \tag{3.15b}$$

together with outer boundary conditions on the channel boundaries,

$$W_0 = 0, \quad Z = -(d/l)\,S/\alpha, (1-d/l)\,S/\alpha. \tag{3.15c}$$

At this stage of the analysis, we recall that $O(U_p^*) = B$ and $O(E) = \alpha\gamma$.

3.3. *Matching*

Having established the outer-region flow, it is necessary to match back to the inner field and it is the result of this further matching which allows the calculation of the inertial migration velocity. Noting that the outer-region momentum equation is driven by the point forcings (3.10), we find that the outer-field velocity has the scalings

$$W_0 \sim \begin{cases} BS & \text{if} \quad \alpha^2/B \ll 1, \\ \alpha S^2 & \text{if} \quad \alpha^2/B \gg 1, \end{cases} \tag{3.16}$$

with the scalings of S given by (3.13). Hence, this implies that the inner velocity field proceeds as

$$w = w_0 + \begin{Bmatrix} BS \\ \alpha S^2 \end{Bmatrix} w_1 + BR_p w_2 + o(R_p), \tag{3.17}$$

where w_1 results from matching the first-order outer field back to the inner field and w_2 results from the regular perturbation expansion of (2.7) (see Appendix C). The first-order inner velocity field, w_1, exerts an additional drag on the particle, modifying its motion and leading to a migration velocity. This velocity is given by evaluating $w_1(r = 1)$. However, making a Taylor series expansion, we note that

$$w_1(r = 1) = w_1(R = S) = w_1(R = 0) + O(S), \tag{3.18}$$

and $w_1(R = 0)$ is just the regular part of the outer velocity field at the origin. Hence, the migration velocity, denoted by $W_{migration}$ is given by

$$W_{migration} = \lim_{R \to 0} \left(W_0 - \begin{cases} (S3/4R)\,(U_p^* + (U_p^* \cdot X/R^2)\,X) \\ -(5S^2/2)\,(X \cdot E \cdot X/R^5) \end{cases} \right). \tag{3.19}$$

	Non-neutrally buoyant $\alpha^2/B \ll 1$	Neutrally buoyant $\alpha^2/B \gg 1$
Shear flow inertia $R_c B^2 \ll 1$	$S^2 = R_p$ $O(W_{migration}) = BR_p^{\frac{1}{2}}$ See §4	$S^2 = R_p$ $O(W_{migration}) = \alpha R_p$ Schonberg & Hinch (1989)
Particle motion inertia $R_c B^2 \gg 1$	$S = R_p B/\alpha$ $O(W_{migration}) = B^2 R_p/\alpha$ See §5, Vasseur & Cox (1977)	No migration at this order Higher-order effects only

TABLE 2. A summary of the scalings for the various parameter regimes in this study. Shear flow inertia denotes the regime in which the far-field balance is between viscous forces and the inertial forces arising from the undisturbed shear flow. Conversely particle motion inertia denotes the regime in which the far-field balance is between viscous forces and inertial forces arising from the flow associated with the motion of the particle.

Higher-order matchings are possible, but this paper focuses on attaining the lowest-order corrections only.

Therefore, we identify four separate cases, because there are two scaling possibilities for both the governing equations and the matching conditions; the values of the non-dimensional parameters ratios $B^2 R_c$ and α^2/B determine which case is appropriate. Furthermore, we consider two alignments of the channel: a vertical channel and an horizontal channel, with gravity acting parallel or perpendicular to the boundaries, respectively. We denote the case $\alpha^2/B \gg 1$ as 'neutrality buoyant particles' and $\alpha^2/B \ll 1$ as 'non-neutrality buoyant particles'. Also, for $R_c B^2 \ll 1$, we denote the problem as a 'shear flow' problem, because the far-field balance is between viscous forces and inertial forces, arising from the undisturbed shear flow. Conversely if $R_c B^2 \gg 1$, the problem is one of a 'quiescent fluid' and the far-field balance is between viscous forces and inertial forces associated with the flow field arising from the buoyancy-induced motion of the particle. We present a summary of the different scalings for each case in table 2. We examine each case in turn, although the neutrally buoyant problems are only briefly discussed below since they have been studied before or are trivially soluble.

3.4. *Neutrally buoyant particles*

The regime in which the strainlet velocity is dominant $(\alpha^2/B \gg 1)$ describes the migration of neutrally buoyant particles. If, in the outer region, viscous forces are balanced by advective terms due to the undisturbed flow $(R_c B^2 \ll 1)$, then this regime corresponds to the case of neutrally buoyant particles $(B = 0)$, studied by Schonberg & Hinch (1989). Their results indicate that the particles migrate across the channel to an equilibrium distance from the plane boundaries. This analysis models the experiments of Segré & Silberberg (1962b), which observe just this migration phenomenon.

If, however, the dominant force balance in the outer region is between viscous forces and inertial forces arising from particle motion $(R_c B^2 \gg 1)$, then we find that there is no migration at this leading-order expansion. This regime requires that $\alpha^2 \gg B \gg R_c^{-\frac{1}{2}}$, which is not compatible with maintaining $\alpha \ll 1$ and $R_c = O(1)$. It turns out that the equations are trivially satisfied and hence there is no lateral motion. Instead, at higher-order corrections we recover the migration effects described above and in §§4 and 5.

4. Non-neutrally buoyant particles in a shear flow: $1 \gg R_c B^2$, $\alpha^2/B \ll 1$

This regime corresponds to the case of the particles having sufficient buoyancy to dominate the far field of the velocity field, but insufficient to affect the outer-region balance of viscous forces with the shear advection term. (This parameter regime is better expressed by the requirement that $R_c^{-\frac{1}{2}} \gg B \gg \alpha^2$.) In essence, the regime corresponds to that first studied by Saffman (1965), although here we generalize his study to include a parabolic velocity profile and the influence of the channel boundaries. Writing $\boldsymbol{W}_0 = (U_0, V_0, W_0)$ and noting the scaling $S^2 = R_p$, we find that the governing equations and boundary conditions are

$$\nabla^2 \boldsymbol{W}_0 - \nabla P_0 = \left(\gamma Z - \frac{4Z^2}{R_c^{\frac{1}{2}}}\right)\frac{\partial \boldsymbol{W}_0}{\partial X} + W_0\left(\gamma - \frac{8Z}{R_c^{\frac{1}{2}}}\right)\hat{\boldsymbol{x}}, \qquad (4.1a)$$

$$\nabla \cdot \boldsymbol{W}_0 = 0, \qquad (4.1b)$$

$$\boldsymbol{W}_0 \sim R_p^{\frac{1}{2}}\frac{3}{4R}\left(\boldsymbol{U}_p^* + \frac{\boldsymbol{U}_p^* \cdot \boldsymbol{X}}{R^2}\boldsymbol{X}\right), \quad |\boldsymbol{X}| \to 0, \qquad (4.1c)$$

$$\boldsymbol{W}_0 = 0, \quad Z = -R_c^{\frac{1}{2}}d/l, R_c^{\frac{1}{2}}(1-d/l). \qquad (4.1d)$$

To enable the calculation of the migration velocity, we consider the regular part of the velocity field at the origin arising from these equations, as discussed in §3.3. Thus

$$\boldsymbol{W}_{migration} = \lim_{R \to 0}\left(\boldsymbol{W}_0 - R_p^{\frac{1}{2}}\frac{3}{4R}\left(\boldsymbol{U}_p^* + \frac{\boldsymbol{U}_p^* \cdot \boldsymbol{X}}{R^2}\boldsymbol{X}\right)\right). \qquad (4.2)$$

We define $\tilde{W}_0$ and $\tilde{P}_0$ to be the two-dimensional Fourier transforms of the disturbance velocity and pressure fields, respectively, in the plane parallel to the channel boundaries,

$$\left\{\begin{matrix}\tilde{W}_0 \\ \tilde{P}_0\end{matrix}\right\} = \frac{1}{4\pi^2}\int_{-\infty}^{\infty}\int_{-\infty}^{\infty}\left\{\begin{matrix}W_0(X, Y, Z) \\ P_0(X, Y, Z)\end{matrix}\right\}e^{-i(k_1 X + k_2 Y)}\,dX\,dY. \qquad (4.3)$$

We then recast the matching condition $(4.1c)$ into the momentum equation by the introduction of a delta-function forcing. The equations for the transformed velocity and pressure fields are then

$$\frac{\partial^2 \tilde{W}_0}{\partial Z^2} - (k_1^2 + k_2^2)\tilde{W}_0 = \begin{pmatrix}ik_1\tilde{P}_0 \\ ik_2\tilde{P}_0 \\ \partial P_0/\partial Z\end{pmatrix} + (\gamma Z - 4R_c^{-\frac{1}{2}}Z^2)ik_1\tilde{W}_0$$

$$+ (\gamma - 8R_c^{-\frac{1}{2}}Z)\tilde{W}_0\hat{X} - \frac{3}{2\pi}R_p^{\frac{1}{2}}\boldsymbol{U}_p^*\delta(Z), \quad (4.4a)$$

$$\frac{\partial^2 P_0}{\partial Z^2} - (k_1^2 + k_2^2)P_0 = -2ik_1(\gamma - 8R_c^{-\frac{1}{2}}Z)\tilde{W}_0 + \frac{3}{2\pi}R_p^{\frac{1}{2}}\boldsymbol{U}_p^*\cdot\begin{pmatrix}ik_1 \\ ik_2 \\ \partial/\partial Z\end{pmatrix}\delta(Z), \quad (4.4b)$$

$$\tilde{W}_0 = 0, \quad Z = -R_c^{\frac{1}{2}}d/l, R_c^{\frac{1}{2}}(1-d/l). \qquad (4.4c)$$

We focus attention on the lateral component of velocity and the pressure field. This gives two coupled differential equations, in which the remaining delta-function forcing

may be replaced by appropriate jump conditions on the velocity and pressure fields at the origin ($Z = 0$). These two governing equations and jump conditions take different forms depending on the alignment of the channel, since this determines the direction of the zeroth-order particle motion U_p^*. We discuss the cases of a vertically and an horizontally aligned channel in the next two subsections. Also, we use the continuity equation (4.1 b) and the no-slip criterion (4.1 d) to provide two boundary conditions for the lateral component of the transformed velocity field on each of the channel boundaries.

4.1. *Horizontally aligned channel*

In this case, the gravitational acceleration is perpendicular to the boundaries and leads to significant zeroth-order lateral motion of the particle. Hence the inertial correction, arising from a consideration of the inertial outer region, will be small. We proceed by setting $U_p^* = B\hat{Z}$ and so the system of equations is

$$\frac{\partial^2 \tilde{W}_0}{\partial Z^2} - (k_1^2 + k_2^2)\,\tilde{W}_0 = \frac{\partial \tilde{P}_0}{\partial Z} + (\gamma Z - 4R_c^{-\frac{1}{2}}Z^2)\,\mathrm{i}k_1\,\tilde{W}_0, \tag{4.5a}$$

$$\frac{\partial^2 \tilde{P}_0}{\partial Z^2} - (k_1^2 + k_2^2)\,\tilde{P}_0 = -2\mathrm{i}k_1(\gamma - 8R_c^{-\frac{1}{2}}Z)\,\tilde{W}_0, \tag{4.5b}$$

$$[\tilde{P}_0]_{Z=0^-}^{Z=0^+} = \frac{3}{2\pi}R_p^{\frac{1}{2}}B, \tag{4.5c}$$

$$\tilde{W}_0 = \frac{\partial \tilde{W}_0}{\partial Z} = 0, \quad Z = -R_c^{\frac{1}{2}}d/l, R_c^{\frac{1}{2}}(1 - d/l). \tag{4.5d}$$

This system of equations is integrated numerically to calculate $\tilde{W}_0(k_1, k_2, 0)$. The correction to the lateral velocity at the origin is obtained by subtracting the two-dimensional Fourier transform of the Stokeslet solution (Appendix B) and inverting,

$$W_{migration} = \mathrm{Re}\left\{\int_{-\infty}^{\infty}\int_{-\infty}^{\infty}\left(\tilde{W}_0(k_1, k_2, 0) - B(R_p)^{\frac{1}{2}}\frac{3}{8\pi}\frac{1}{(k_1^2 + k_2^2)^{\frac{1}{2}}}\right)\mathrm{d}k_1\,\mathrm{d}k_2\right\}. \tag{4.6}$$

In this expression Re denotes the real part and we note that $W_{migration}$ is an $O(BR_p^{\frac{1}{2}})$ correction to the particle velocity.

As $k_1, k_2 \to \infty$, we expect that the solution of (4.5) should recover the Stokeslet velocity field, simply because large Fourier modes correspond to short lengthscales which are not influenced by the presence of the plane boundaries. The system of equations (4.5) may be examined in this limit (Appendix D) and it is found that

$$\tilde{W}_0(k_1, k_2, 0) = BR_p^{\frac{1}{2}}\frac{3}{8\pi(k_1^2 + k_2^2)^{\frac{1}{2}}} + O((k_1^2 + k_2^2)^{-\frac{3}{2}}). \tag{4.7}$$

This result guarantees the convergence of (4.6), although it is possible that $\tilde{W}_0(k_1, k_2, 0)$ must be evaluated for large values of $(k_1^2 + k_2^2)^{\frac{1}{2}}$. The numerical evaluation of the inversion integral (4.6) was carried out in the (k_1, k_2)-plane using plane polar coordinates, restricting attention to the first quadrant, owing to a symmetry of $\mathrm{Re}(\tilde{W}_0)$.

NAG routines (D02RAF, C05NBF, D01DAF) were used to solve finite-difference versions of the system of differential equations and to evaluate the Fourier inversion integral. Some difficulty was experienced in obtaining convergence for large values of $(k_1^2 + k_2^2)$. Equations (4.5) admit both exponentially growing and decaying solutions
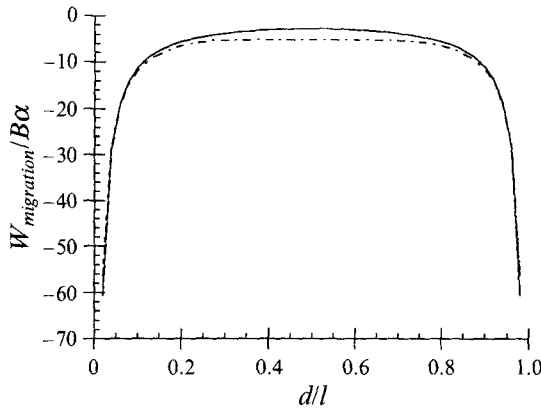
FIGURE 2. The correction to the sedimentation velocity versus lateral position, for a non-neutrally buoyant particle in an horizontal shear flow for $R_c = 0.01$ (---), $R_c = 1.0$ (——) and $R_c = 100$ (-·-·-).

whereas the boundary conditions require the decaying solution. It becomes hard to resolve the decaying solution as the Fourier mode number increases and the exponentially growing solution starts to dominate and interfere with the relaxation techniques of the finite-difference grid. Hence the asymptotic expression for the velocity field was used for large Fourier modes.

The correction to the sedimentation velocity ($W_{migration}$) is calculated across the channel for $R_c = 0.01, 1.0, 100$ and it is observed to always reduce the velocity of the particles towards the boundaries. The results are shown in figure 2 and for the purposes of displaying these results, we plot the migration velocity on an axis scaled with αB. It is noted that the three curves take similar values with this scaling; only when $R_c = 100$ does the migration velocity show a slightly different variation across the channel width. The correction is not calculated within $0 < d/l < 0.04$ and $0.96 < d/l < 1$: these correspond to locations near the plane boundaries and convergence difficulties arise. Furthermore, within these regions close to the boundaries it is unlikely that the analysis presented here is valid because the boundary is not sufficiently distant from the particle. The inertial contribution to the migration velocity across the streamlines is not dependent upon the direction of the undisturbed channel flow or whether the buoyancy induces upward or downward motion. Instead the inertial effect, at first-order, is always to reduce the migration velocity by increasing the drag on the particle.

4.2. Vertically aligned channel

In this case the gravitational acceleration is parallel to the streamlines of the undisturbed flow and so there is no zeroth-order lateral motion of the particle arising from the Stokesian region. Hence the inertial correction, although of small magnitude, dominates the lateral motion. We set $U_p^* = B\hat{X}$ and find that the system of equations is given by (4.5a, b, d), but with the jump condition replaced. In this regime, the jump condition is

$$\left[\frac{\partial \tilde{P}_0}{\partial Z}\right]_{Z=0^-}^{Z=0^+} = ik_1 \frac{3}{2\pi} BR_p^{\frac{1}{2}}. \tag{4.8}$$

As in §4.1, we numerically integrate this system of equations to calculate $\tilde{W}_0(k_1, k_2, 0)$. The lateral velocity is given by inverting this expression because there is no
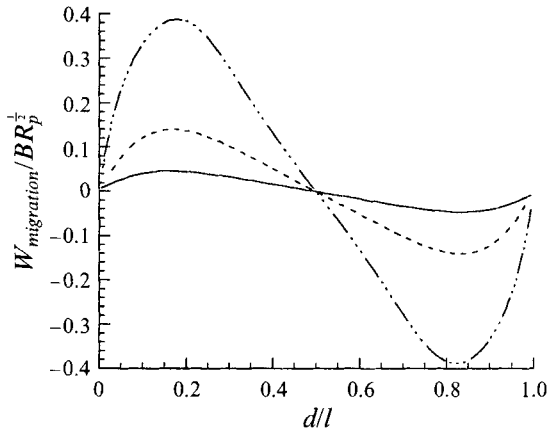
FIGURE 3. Migration velocity versus lateral position of a non-neutrally buoyant particle in a vertical shear flow for $R_c = 1.0$ (——), $R_c = 10$ (---), $R_c = 100$ (—···).

contribution from the Fourier transform of the Stokeslet solution, as demonstrated in Appendix B. Hence

$$W_{migration} = \text{Re}\left\{ \int_{-\infty}^{\infty} \int_{-\infty}^{\infty} \tilde{W}_0(k_1, k_2, 0)\,dk_1\,dk_2 \right\}. \tag{4.9}$$

As before, we note that $W_{migration}$ is $O(BR_p^{\frac{1}{2}})$. An asymptotic analysis of (4.6 a, b, d), (4.8) for large Fourier mode number (Appendix D) shows that

$$\tilde{W}_0 = -BR_p^{\frac{1}{2}}\frac{3\gamma}{16\pi}\frac{k_1^2}{(k_1^2+k_2^2)^{\frac{5}{2}}}+O((k_1^2+k_2^2)^{-\frac{5}{2}}). \tag{4.10}$$

This guarantees the convergence of (4.9) and is used to evaluate the integral and to avoid convergence problems of integrating the finite-difference equations at large Fourier mode number. We use a similar numerical scheme to that described in §4.1, again restricting attention to the first quadrant of the (k_1, k_2)-plane. The lateral migration was calculated for $R_c = 1.0, 10, 100$ and the velocities across the channel width are shown in figure 3. We find that these curves have the same generic form, with the migration velocity being single, but differently signed in each half of the channel. There is a maximum migration velocity at $d/l \approx 0.15$ (0.85) and zero migration velocity at the channel centre. Once again, we did not evaluate the migration velocity near to the channel boundaries, owing to difficulties in achieving convergence of the numerical scheme.

We note that reversing the buoyancy of the particle ($B \rightarrow -B$), or reversing the direction of the undisturbed channel flow ($\bar{u}^* \rightarrow -\bar{u}^*$) leads to a reversal of the direction of migration. These symmetries imply that if the buoyancy of the particle leads to motion in the same direction as the undisturbed flow, then the lateral migration is outward, towards the boundaries. Conversely, if the buoyancy leads to motion opposed to the direction of the undisturbed flow, then the migration is towards the channel centre. This behaviour is in accord with the analysis of Saffman (1965), but is in contrast to that of a neutrally buoyant particle, for which there exists an equilibrium position away from the channel centreline and towards which the particles migrate. This observation will be further discussed in §6, where all the results are reviewed.

5. Non-neutrally buoyant particles in quiescent fluid: $1 \ll R_c B^2$, $\alpha^2/B \ll 1$

In this regime, the buoyancy of the particle is sufficient to dominate motion as it sediments through the shear flow and to dominate the outer-region balance between viscous and advective terms. This analysis is similar to that of Oseen, which describes the motion of a sphere through an unbounded quiescent fluid. Here, although the shear rate of the undisturbed flow is sufficiently small so that to leading order the fluid may be treated as quiescent, it is not unbounded and so the channel boundaries influence the motion.

We may solve the quasi-steady-state equations for only the case of a vertically aligned channel. For an horizontally aligned channel, the gravitational acceleration leads to significant motion across the streamlines. We have derived the constraint (3.12) to permit the time variation to be neglected which is not consistent with requiring $R_c B^2 \gg 1$ and $R_c = O(1)$. In other words, the particle moves towards the boundary before the disturbance velocity field has been fully established across the channel. Hence a quasi-steady approximation is inappropriate and the momentum equation must include the time-derivative term.

The vertically aligned channel in the absence of an undisturbed flow was analysed by Vasseur & Cox (1977), using a method similar to the one presented here. The undisturbed shear flow is present but is dominated by the particle's sedimentation. There is the possibility, though, that the weak shear may influence the lateral migration, which is elucidated through the scalings developed here. Using the outer coordinate scaling $S = R_p B/\alpha$ and identifying $U_p^* = B\hat{X} + O(\alpha^2)$, we find that the system of equations is

$$\nabla^2 W_0 - \nabla P_0 = -U_p^* \cdot \nabla W_0, \tag{5.1a}$$

$$\nabla \cdot W_0 = 0, \tag{5.1b}$$

$$W_0 \sim \frac{3BR_p}{4\alpha R}\left(U_p^* + \frac{U_p^* \cdot X}{R^2}X\right), \quad |X| \to 0, \tag{5.1c}$$

$$W_0 = 0, \quad Z = -BR_c d/l, BR_c(1-d/l). \tag{5.1d}$$

Once again, we are interested in the regular part of the velocity field at the origin arising from these equations. This is given by

$$W_{migration} = \lim_{R \to 0}\left(W_0 - \frac{R_p B}{\alpha}\frac{3}{4R}\left(U_p^* + \frac{U_p^* \cdot X}{R^2}X\right)\right). \tag{5.2}$$

This drives an $O(R_p B^2/\alpha)$ term in the inner velocity field which leads to lateral migration. However, the calculations of Appendix C demonstrate that there is also a regular perturbation term. This is of $O(R_p B)$ and also leads to particle migration. This regular perturbation term can only dominate the singular perturbation correction if $B/\alpha \ll 1$ and within the strict parameter regime imposed here this is not a possibility. However, it may have a contribution with intermediate parameter regimes, which fall between those analysed in §§4 and 5.

We recalculate the results of Vasseur & Cox (1977) using the method of Fourier transforms in the plane parallel to the channel. The system of equations is linear with constant coefficients and so is easily integrated. Typical results are shown in figure 4. There are two noteworthy features of these results. Firstly, as pointed out by Vasseur & Cox (1977), the migration velocity tends to the asymptotic value of $\frac{3}{32}R_p B^2/\alpha$ as the particle approaches the boundary. This result is in accord with that calculated by Cox
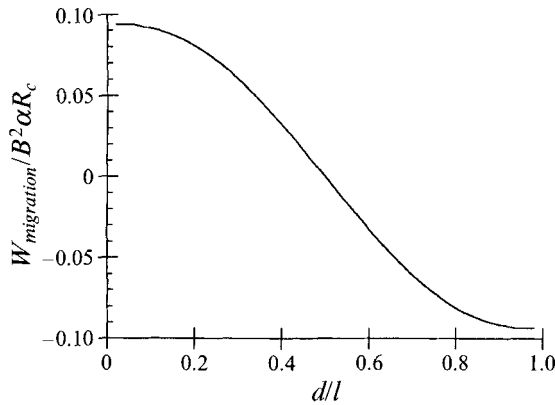
FIGURE 4. Migration velocity versus lateral position for a non-neutrally buoyant particle within a channel with quiescent fluid, for $R_c = 1.0$.

& Hsu (1977) in which they assumed that a single boundary fell within the inner Stokesian layer, and may be reproduced from this analysis by integration of (5.1) in the limit $d/l \to 0$. Also, and somewhat trivially, the migration is always directed towards the channel centreline, irrespective of the sign of the particle's buoyancy, which is in contrast to the study of §4.2.

6. Discussion

This paper has studied the inertial correction to the motion of a small spherical particle in the direction perpendicular to the streamlines of the undisturbed flow. The sphere is non-neutrally buoyant and we have considered the cases where the buoyancy-induced zeroth-order motion is parallel or perpendicular to the undisturbed streamlines, corresponding to the alignment of the channel being vertical or horizontal. The major new results of this paper correspond to the parameter regime $R_c B^2 \ll 1$, $\alpha^2/B \ll 1$ and are presented in §4.

When the channel is aligned horizontally and the particle moves perpendicularly across the flow towards the boundaries, the inertial correction to the Stokes' settling velocity is small, as calculated in §4.1. The analysis shows that the correction is of $O(BR_p^{\frac{1}{2}})$. This scaling is identical to that calculated by Harper & Chang (1968) in their extension to the analysis of Saffman (1965). Whereas Saffman (1965) considered the lift on a particle moving parallel to the streamlines of an unbounded linear shear flow, Harper & Chang (1968) calculated the lift and drag on a body moving in an arbitrary direction through the same unbounded shear flow. Their results may be derived from this study by taking the limit $l \to \infty$, while $Re_s = \alpha B R_c$ and $\Gamma = U_m/l$ remain finite. However, this study also includes the influence of the boundaries on the particle motion. We have also shown that the drag on the particle is increased, irrespective of the sign of the velocity gradient. This feature is unlike the 'Saffman lift', the direction of which reverses with differing signs of shear. (Appendix E revises the Harper & Chang calculation to include the dependence on the direction of increasing velocity.) This increase of particle drag is expected, since we deduce from the minimum-dissipation theorem for creeping flow that the introduction of any inertial terms must indeed lead to an increased drag (Happel & Brenner 1965).

Several studies (e.g. Brenner 1961; Ho & Leal 1974) have demonstrated that a particle moving perpendicularly towards a boundary experiences an additional drag,
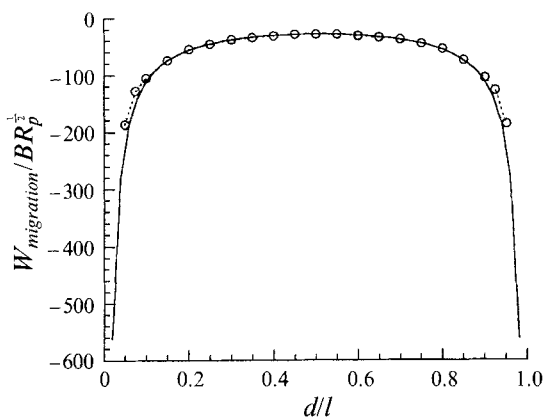
FIGURE 5. Comparison of the correction to the sedimentation velocity of a non-neutrally buoyant particle in an horizontal shear flow, between the results of Ganatos *et al.* (1980) (--○--) and the results for $R_c = 0.01$ (——).

which reduces the particle's velocity. This effect arises both in creeping flow and when inertia is taken into account. It implies that for the problem studied in §4.1 there are two means by which the velocity of the particle towards the boundary is reduced – one resulting from the viscous interaction with the boundary and the other from the introduction of inertia.

Using the scalings developed in §3 for a non-neutrally buoyant particle with an outer-region balance of the viscous and shear inertial terms, we find that the dimensional distance from the boundary at which inertia becomes significant is given by

$$\Delta \sim a/S = l/R_c^{\frac{1}{2}}.$$

Thus for $R_c < 1$, the particle wake fills the entire width of the channel and the boundaries, which fall within the Stokesian region, dominate the motion. Conversely, for $R_c > 1$, the central regions of the channel are dominated by the shear inertial correction and the boundary influence is limited to distances $O(l/R_c^{\frac{1}{2}})$. This qualitative feature is observed in figure 2, for $R_c = 100$. Here the wall effect is significant for $\{d/l < 0.1, \ d/l > 0.9\}$, with the remainder dominated by an inertial correction comparable to that calculated by Harper & Chang (1968) with a non-dimensional shear rate of order unity.

The results for $R_c = 0.01$ show an increased particle drag which is dominated by viscous–boundary interactions. This calculation may be compared to other creeping-flow evaluations of the boundaries' influence. Brenner (1961) presented an 'exact' one-boundary solution, while both Ganatos *et al.* (1980) and Ho & Leal (1974) studied the problem of a particle moving perpendicularly between two boundaries. There is good agreement between the results calculated here and those of Ganatos *et al.* (1980) (see figure 5), while those of Ho & Leal (1974), using a method of reflections, tend to underestimate the additional drag. (Ganatos *et al.* suggest that this underestimation indicates a need to take additional terms in the reflection series.)

When the particle's buoyancy leads to motion parallel with the boundaries, the inertial correction will produce the leading-order lateral motion. The results of §4.2, which are calculated for the regime of $R_c B^2 \ll 1$, $\alpha^2/B \ll 1$, demonstrate that a particle whose buoyancy enhances motion in the direction of the undisturbed flow will migrate towards the boundaries, whereas a particle whose buoyancy is in opposition to the

direction of the undisturbed flow will migrate towards the channel centreline. (For example, the former condition is fulfilled by a light particle in an upward flow, whereas the latter by a heavy particle in an upward flow.) This migration velocity is $O(B\alpha R_c^{\frac{1}{2}})$ and the variation across the channel width is shown in figure 3. We find a similar variation of migration velocity across the width of the channel in the experimental study of Jeffrey & Pearson (1965) and discuss their results below.

The direction of the inertial migration is in accord with that predicted by Saffman (1965). A particle moving faster than the background shear flow will migrate in the direction of slower flow (i.e. in the direction of decreasing velocity), and vice versa. A simple physical argument to account for the direction of this migration is that as the particle translates parallel to the boundaries it displaces fluid laterally. At sufficiently large distances this displacement becomes irreversible, owing to the effect of inertia. If the particle lags the fluid, the difference between the velocity of the displaced fluid and the background flow is greater in the direction of increasing velocity. Hence a lateral pressure gradient is set up in this direction which exerts a force on the particle that leads to migration. (A reverse argument applies for a particle translating with velocity in excess of the background fluid and so it migrates in the direction of decreasing velocity.)

If the undisturbed shear flow is weak ($R_c B^2 \gg 1$), we find that the lateral migration is $O(\alpha B^2 R_c)$ and is always directed towards the channel centreline. This effect was first calculated by Vasseur & Cox (1977) and a simple physical explanation of this migration given by McLaughlin (1993). As the particle translates through the fluid, between the boundaries, it displaces fluid laterally and inertial effects imply that this is irreversible at sufficiently large distances from the particle. The boundaries encounter and resist this displacement of fluid and exert a force on the particle, which leads to migration towards the centreline. It is vital that the boundaries are sufficiently distant to lie within the outer region in which inertia terms are important, as this adds irreversibility to fluid displacement. We note that the magnitude of these migration velocities decrease with decreasing channel Reynolds numbers, which is in accord with this reasoning.

Schonberg & Hinch (1989) note that the migration of neutrally buoyant particles arises from the competition of two effects: one is linked to inertial interaction with the wall, which produces inward drift, and the other is linked to the shear and curvature of the velocity profile, which leads to migration towards the boundaries. The simple physical arguments presented above explain both of these effects. To zeroth-order, a neutrally buoyant particle does not lag behind the channel flow and so if there is a linear shear flow no lateral pressure gradient arises and so there is no migration. However, there is curvature in the velocity profile across the channel and so, at large distances from the particle, the difference between the velocity of displaced and background fluid is greater towards the boundary than towards the channel centre. This induces a pressure gradient and leads to migration towards the boundary. Conversely, the boundary encounters and resists irreversibly displaced fluid and exerts a force on the particle, which leads to migration away from it.

A number of questions arising from the experiments of Jeffrey & Person (1965) may be answered by this theoretical study of inertial migration effects. Firstly, when studying the migration of non-neutrally buoyant particles, Jeffrey & Pearson scale the migration velocity with $\alpha^2 B R_c$, although they note the empirical result that improved correlation arises from scaling with $(\alpha B R_c)^{\frac{1}{2}}$. The analysis of §4.2 suggests that if the particles are in the parameter regime $\alpha^2/B \ll 1$, $R_c B^2 \ll 1$, the scaling should be $\alpha B R_c^{\frac{1}{2}}$. Furthermore, the scaling for the migration velocity of neutrally buoyant particles should be $\alpha^3 R_c$, as suggested by Segré & Silberberg (1962 *a*, *b*), rather than $\alpha^2 R_c^{\frac{1}{2}}$ which
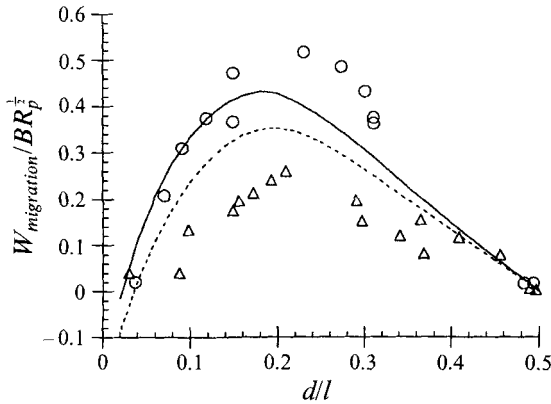
FIGURE 6. Comparison of the migration velocity versus lateral position between theoretical predictions and experimental results of Jeffrey & Pearson (1965). Two data sets are shown: $R_c B^2 = 0.07$, $B/\alpha^2 = 9.60$ (O, —), $R_c B^2 = 0.14$, $B/\alpha^2 = 18.80$ ($\triangle$, ---).

arises from Jeffrey & Pearson's correlation analysis. If we compute the ratios α^2/B and $R_c B^2$ for the data set of Jeffrey & Pearson (1965), it turns out that the experiments were conducted in a parameter regime which does not strictly satisfy the criterion $\alpha^2/B \ll 1$, $R_c B^2 \ll 1$, although generally $\alpha^2/B < 1$ and $R_c B^2 < 1$. Hence, although the dominant behaviour may be predicted by the analysis in the regime of §4.2, it is also necessary to include 'intermediate' effects from other limiting regimes. Their experiments with non-neutrally buoyant particles were performed using dense particles in upward and downward flow. In the upward flow, there is migration towards the tube axis, whereas in downward flow there is migration towards the boundaries. However, the magnitude of these migration velocities for the upward and downward flows does not exhibit the same distribution across the tube, which the theory of §4.2 predicts. A possible reason for this discrepancy could be related to the migration effects described in §5. In the regime of $R_c B^2 \gg 1$, which corresponds to a regime of quiescent fluid, all particles migrate inwards to the channel centreline. In these experiments, $R_c B^2 = O(1)$ and so behaviour from the quiescent fluid and shear flow regimes will be observed. Hence, the inward migration of dense particles in an upward flow will be enhanced, while in a downward flow the outward migration is diminished. This effect would explain the observed discrepancy in the tube velocity profiles for heavy and light particles observed by Jeffrey & Pearson.

We compare the theoretical predictions of §4 with some of the experimental results presented by Jeffrey & Pearson (1965). The governing equations are integrated with appropriate values of the non-dimensional parameters, to give the migration velocity across the channel (figure 6). We find general qualitative agreement between the experimental and theoretical velocity profiles, although there is not quantitative agreement across the entire width of the channel. This may arise from the difference between the planar symmetry of the channel in the theoretical calculation and the cylindrical tube used for the experiments. Furthermore, the experiments were performed in the regime $R_p/\alpha = O(1)$, which is not strictly in accord with the analysis developed here. Nevertheless, we do find at least some experimental verification of the theoretical predictions.

We conclude this discussion of the analysis of particle migration by considering regimes in which there is an equilibrium position across the channel width at which the lateral migration velocity vanishes. The observations of Segré & Silberberg (1962 *a, b*)
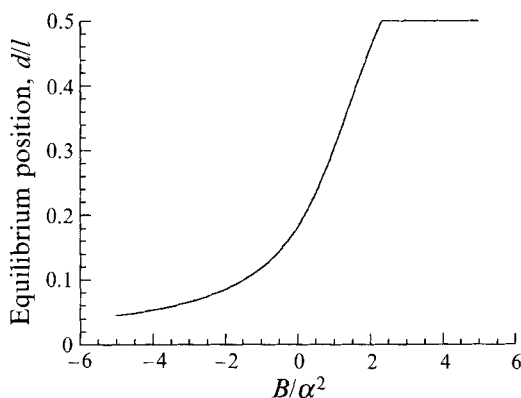
FIGURE 7. The variation of equilibrium position with B/α^2 for a particle in a vertical shear flow with $R_c = 1.0$.

that such an equilibrium position exists away from the channel centreline initiated much of the work on inertial migration effects. Schonberg & Hinch (1989) calculate the equilibrium position for a neutrally buoyant particle and their analysis finds it to be at $d/l = 0.185$ for $R_c = 1.0$. This value is in accord with experimentally determined equilibrium positions. Their calculations are in the parameter regime $\alpha^2/B \gg 1$, $R_c B^2 \ll 1$.

Vasseur & Cox (1977) study the case of a non-neutrally buoyant particle in quiescent fluid, with a channel Reynolds number of order unity. This corresponds to the parameter regime $\alpha^2/B \ll 1$, $R_c B^2 \gg 1$. They find that the particles migrate towards the channel centreline. The work presented in this paper has studied non-neutrally buoyant particles in a shear flow and we find that migration can be towards either the channel boundaries or centreline, depending on the buoyancy and the direction of flow. The parameter regime of §4 is $\alpha^2/B \ll 1$, $R_c B^2 \ll 1$ and so it is possible to consider intermediate effects with the inertial migrations described by Schonberg & Hinch (1989) and Vasseur & Cox (1977).

Firstly, we describe a regime in which shear flow dominates, but in which the particle is only slightly non-neutrally buoyant ($\alpha^2/B = O(1)$, $R_c B^2 \ll 1$). For definiteness, we consider a vertically aligned channel with an upward flow. Hence light particles migrate outwards and heavy particles inwards, according to the theory of §4.2. Thus combining these migration effects with those of Schonberg & Hinch (1989), we find that for light particles the equilibrium position is moved towards the channel boundaries, whereas for heavy particles the equilibrium position gradually moves inwards to the centreline with increasing B/α^2. The location of this equilibrium position is calculated for a range of B/α^2 and is shown in figure 7. For extremely light particles, the equilibrium position is close to the boundary; since the analysis is not entirely valid with the particle adjacent to the boundary, we should include additional effects to study possible equilibrium positions here.

An equilibrium is also possible in the regime of non-neutrally buoyant particles with weak shear flows ($\alpha^2/B \ll 1$, $R_c B^2 = O(1)$). Here the inward migration predicted by Vasseur & Cox (1977) is balanced by the outward migration predicted by §4.2. We discuss a vertically aligned channel with upward flow and light particles ($B < 0$), which implies that the particles migrate outwards according to the §4.2. We consider the variation of the equilibrium position with the ratio of the two migration velocity scales, $B\alpha R_c^{\frac{1}{2}}/B^2 \alpha R_c$ (figure 8). We calculate the equilibrium position by solving the system of
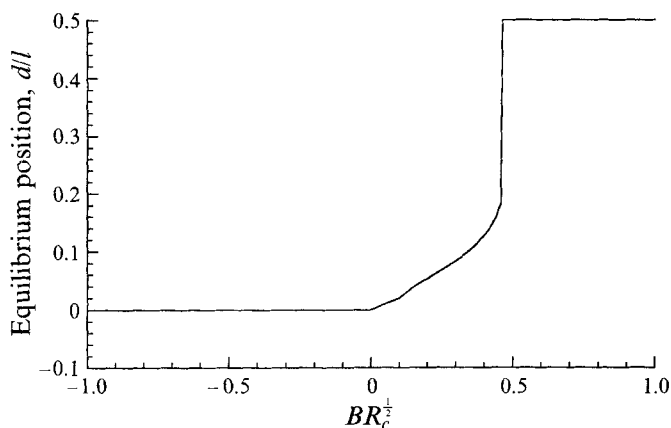
A. J. Hogg

FIGURE 8. The variation of equilibrium position with $BR_c^{\frac{1}{2}}$ for a non-neutrally buoyant particle in a vertical channel with $R_c = 1.0$.

equations for the lateral velocity field at each value of $BR_c^{\frac{1}{2}}$ and finding the position at which the migration velocity vanishes. We find that for large values of $BR_c^{\frac{1}{2}}$, the centreline of the channel is the equilibrium position since the 'quiescent fluid' solution dominates. However, the position moves towards the boundaries at $BR_c^{\frac{1}{2}} \approx 0.50$ and therefore gradually approaches the boundary with decreasing $BR_c^{\frac{1}{2}}$. Here the 'shear flow' solution begins to dominate. We find that there are equilibrium positions between $0.2 \leqslant d/l \leqslant 0.5$, for only a very limited range of values for $BR_c^{\frac{1}{2}}$. This result is in accord with the findings of Vasseur & Cox (1976) at low channel Reynolds number and may account for the lack of experimental observations of equilibrium at these channel widths.

Finally, we return to an horizontally aligned channel and consider a slightly non-neutrally buoyant particle. The lateral motion is $O(B)$ with inertial corrections $O(BR_p^{\frac{1}{2}})$ arising from the Stokeslet term and $O(\alpha R_p)$ from the strainlet term. It is feasible that $B \sim \alpha R_p$, in which case there is an equilibrium position at some distance from the channel centreline, but nearer the boundary than for a neutrally buoyant particle. The location of this equilibrium position may be extracted directly from the results of Schonberg & Hinch (1989), again with the caveat that close to the boundary the analysis is not likely to be entirely valid.

7. Application

The geometry and flow of the problem of an horizontally aligned channel are identical to that encountered in the technique of field-flow fractionation (FFF) (Giddings *et al.* 1991). This technique is used to separate particles of differing sizes and densities and is generally carried out in a channel which is relatively thin and long. The channel Reynolds number is small and the flow has a Poiseulle profile. The essence of FFF is to apply a field perpendicular to the flow which induces particle motion and drives some of the particles closer to the boundaries than others. Those close to the boundaries are now transported more slowly by the flow, which allows separation to be effected. A sedimentation field is commonly used for FFF. However, while gravity has been successfully used for particles with diameters in excess of 1 µm, it is usual to generate sedimentation forces for smaller particles by using a centrifuge (Giddings *et al.* 1991).

The analysis here is relevant to the technique of sedimentation fluid flow fractionation, as we have studied a motion-inducing field applied perpendicular to the channel flow. The analysis demonstrates that particles that sediment towards a boundary across the shear flow experience an increased drag force, which slows their rate of sedimentation. For the purposes of predicting particle motions within FFF, this means that it may not be adequate to assume that the particle sediments with the Stokes' settling velocity. Instead there are inertial corrections $O(BR_p^{\frac{1}{2}})$ and $O(\alpha R_p)$. Hence, we conclude that for particles which differ in size alone, the difference between their sedimentation velocities is reduced.

A second application of this work may be in connection with particle motions near to an erodible bottom boundary in open channel flow. Abbott & Francis (1977) note that the grains they tracked seemed to sediment more slowly than predicted by the Stokes' settling velocity. This indicates an additional upward force which may be ascribed to a shear–inertial lift. Their experiments were carried out at a moderate channel Reynolds number as they wished to study particle motions in the absence of turbulence. For modelling their experiments, it may be possible therefore to extend this analysis to the appropriate parameter regime, which is an open channel flow at a Reynolds number of 400. In turbulent systems, the analysis may not be applied directly, as we have assumed that the background flow is steady and laminar and have used a simplified equation of motion for the particles, which assumes small inertial forces and neglects turbulent fluctuations and particles' wakes. However, it may be possible to apply the principle that the particles experience a 'lift force' near to the boundary and so their concentration is reduced in this region.

Finally, we describe how this work may be applied to volcanic conduits, up through which molten rock (or magma) is flowing. The flow within such dykes is often laminar and we may calculate a typical channel Reynolds number, using data from Lister & Kerr (1991). If the magma is basaltic, with viscosity $100 \, \mathrm{Pa \, s^{-1}}$ and density $2600 \, \mathrm{Kg \, m^{-3}}$, flowing through a dyke of width 0.5 m, with a velocity of $1 \, \mathrm{m \, s^{-1}}$, then the channel Reynolds number falls in the regime $R_c = O(10)$. It is observed that small bubbles migrate across the dyke, towards the boundaries (Brousse 1965). The direction of this observed migration is in accord with the calculations made here for a vertically aligned channel. However, in addition to this inertia-driven migration, it is also possible that bubbles migrate due to deformation. The shear deforms the shape of the bubbles and leads to migration towards the channel centre. This deformation will be significant when the surface tension of the bubble is small compared to the viscous forces acting on it, which tends to be the case for larger bubbles. The calculations of §4.2 also suggest that crystals in volcanic conduits, which are heavier than the flowing magma, should migrate towards the channel centre. This has not been observed, possibly because the thermal effects of a lateral temperature gradient are important or because the crystals have an irregular shape leading to other mechanisms of lateral migration.

Appendix A

In this appendix, we present the solution to the creeping-flow problem with a quadratic boundary condition on the sphere, at the origin, which is required to solve the inner problem of §3.1. We consider the following non-dimensional equations and boundary conditions:

$$\nabla^2 \boldsymbol{u} - \nabla p = 0, \qquad \nabla \cdot \boldsymbol{u} = 0, \qquad (A\,1a, b)$$

$$\boldsymbol{u} = 4\alpha^2 z^2 \hat{\boldsymbol{x}}, \quad r = 1, \qquad \boldsymbol{u} \to 0, \quad r \to \infty, \qquad (A\,1c, d)$$

where $r = |\boldsymbol{x}|$. We solve the problem in terms of spherical harmonics and define a system of spherical polar coordinates (r, θ, ϕ), with the axis $\theta = 0$ aligned along the x-axis of the Cartesian system. Hence, the boundary condition (A 1c) is given by

$$\boldsymbol{u} = 2\alpha^2 \sin^2 \theta \, (\cos 2\phi + 1)(\cos \theta \hat{\boldsymbol{r}} - \sin \theta \hat{\boldsymbol{\theta}}), \qquad (A\,2)$$

where $\hat{\boldsymbol{r}}, \hat{\boldsymbol{\theta}}, \hat{\boldsymbol{\phi}}$ are unit basis vectors of the spherical coordinate system. Noting the harmonics of this boundary condition, we seek a solution for the velocity and pressure fields in terms of the following spherical harmonics:

$$\boldsymbol{u}/\alpha^2 = \nabla \psi_{-2}^0 + \nabla \psi_{-4}^0 + \nabla \psi_{-4}^2 + \boldsymbol{x} \wedge \nabla \chi_{-3}^2$$
$$+ r^2 (\nabla p_{-2}^0 + \tfrac{1}{15} \nabla p_{-4}^0 + \tfrac{1}{15} \nabla p_{-4}^2) + \boldsymbol{x}(4p_{-2}^0 - \tfrac{8}{15}(p_{-4}^0 + p_{-4}^2)), \qquad (A\,3a)$$

$$p/\alpha^2 = 2(p_{-2}^0 + p_{-4}^0 + p_{-4}^2), \qquad (A\,3b)$$

where the decaying spherical harmonics are denoted by

$$\{\psi_{-(n+1)}^m, p_{-(n+1)}^m, \chi_{-(n+1)}^m\} = r^{-(n+1)} P_n^m(\cos \theta) \, e^{im\phi},$$

and $P_n^m(z)$ are the Legendre polynomials. After some algebra, we pick out the following harmonics which solve this problem:

$$\psi_{-2}^0 = \frac{3}{5r^2} \cos \theta, \quad \psi_{-4}^0 = -\frac{5 \cos^3 \theta - 3 \cos \theta}{4r^4}, \quad \psi_{-4}^2 = \frac{5}{4r^4} \cos \theta \sin^2 \theta \cos 2\phi, \quad (A\,4a\text{--}c)$$

$$p_{-2}^0 = \frac{1}{r^2} \cos \theta, \quad p_{-4}^0 = \frac{7(5 \cos^3 \theta - 3 \cos \theta)}{4r^4}, \quad p_{-4}^2 = -\frac{35}{4r^4} \cos \theta \sin^2 \theta \cos 2\phi, \quad (A\,4d\text{--}f)$$

$$\chi_{-3}^2 = \frac{2}{3r^3} \sin^2 \theta \sin 2\phi. \qquad (A\,4g)$$

These give the velocity field $\boldsymbol{u} = \alpha^2 (u_r, u_\theta, u_\phi)$ as

$$u_r = \cos \theta \sin^2 \theta \cos 2\phi \left(-\frac{5}{r^5} + \frac{7}{r^3}\right) + \cos^3 \theta \left(\frac{5}{r^5} - \frac{7}{r^3}\right) + \cos \theta \left(-\frac{3}{r^5} + \frac{3}{r^3} + \frac{2}{r}\right), \qquad (A\,5a)$$

$$u_\theta = \sin^3 \theta \cos 2\phi \left(-\frac{15}{4r^5} + \frac{7}{4r^3}\right) + \sin \theta \cos 2\phi \left(\frac{5}{2r^5} - \frac{5}{2r^3}\right)$$
$$+ \sin^3 \theta \left(-\frac{15}{4r^5} + \frac{7}{4r^3}\right) + \sin \theta \left(-\frac{1}{r} - \frac{2}{r^3} + \frac{3}{r^5}\right), \qquad (A\,5b)$$

$$u_\phi = \sin \theta \cos \theta \sin 2\phi \left(-\frac{5}{2r^5} + \frac{5}{2r^3}\right). \qquad (A\,5c)$$

The force and couple exerted on the sphere by this flow, denoted by $\boldsymbol{F}$ and $\boldsymbol{G}$ respectively, are simply calculated from these spherical harmonics (Happel & Brenner 1965) as

$$\boldsymbol{F} = -4\pi\alpha^2 \nabla(2r^3 p_{-2}^0) = -8\pi\alpha^2 \hat{\boldsymbol{x}}, \quad \boldsymbol{G} = 0. \qquad (A\,6a, b)$$

We note that the force and couple may also be calculated using Faxén's formula, which yields an exact result in this case as the background flow is quadratic.

Appendix B. Stokeslet and strainlet velocity fields

In this appendix, we derive the Stokeslet and strainlet velocity fields and calculate their two-dimensional Fourier transforms, evaluated at the origin, in the plane parallel to the boundaries of the channel. These expressions are used in the matching procedure of §3.3.

B.1. *Stokeslet*

The Stokeslet velocity field is defined as that resulting from the introduction of a delta-function forcing in the momentum equation. It is equivalent to the far-field terms of the velocity field for an object translating through quiescent fluid. Its analytical form may be derived from the zero-Reynolds-number Navier–Stokes equations, using Fourier transforms. For a forcing of magnitude F at the origin, we find that the non-dimensional Stokeslet velocity and pressure fields are given by

$$p(x) = \frac{1}{4\pi} \frac{F \cdot x}{r^3}, \quad u_j(x) = \frac{1}{8\pi} F_i \left(\delta_{ij} + \frac{x_i x_j}{r^2} \right). \tag{B 1a, b}$$

As part of the asymptotic matching procedure of §3.3, we need to calculate the two-dimensional Fourier transform of this Stokeslet velocity field evaluated at $z = 0$. Writing $K^2 = k_1^2 + k_2^2$, we find that the two-dimensional Fourier transform of the Stokeslet velocity field, in the plane (x, y), evaluated at the origin is

$$\hat{u}_i(k_1, k_2) = \frac{1}{8\pi^2 K} (F_i - \tfrac{1}{2} \Lambda_{ij} F_j), \tag{B 2}$$

where

$$\Lambda = \begin{pmatrix} k_1^2/K^2 & k_1 k_2/K^2 & 0 \\ k_1 k_2/K^2 & k_2^2/K^2 & 0 \\ 0 & 0 & 1 \end{pmatrix}.$$

B.2. *Strainlet*

The Strainlet velocity field is defined as that resulting from forcing the creeping-flow momentum equation with a linear combination of derivatives of the delta function. The forcing takes the form $\frac{20}{3}\pi E_{ij}(\partial/\partial x_j)\,\delta(x)$, where E_{ij} is symmetric and traceless. It is equivalent to the far-field term for a stationary object at the origin of a linear shear flow. Its analytical form is also derived from the creeping flow equations by Fourier transforms and we find that the non-dimensional velocity and pressure fields are given by

$$p(x) = \frac{5x_l E_{lj} x_j}{6r^3}, \quad u_m(x) = \frac{5}{2} \frac{x_l E_{lj} x_j}{r^5} x_m. \tag{B 3a, b}$$

Thus we calculate the two-dimensional Fourier transform of this velocity field, evaluated at the origin. Denoting $K^2 = k_1^2 + k_2^2$, we find

$$\hat{u}(k_1, k_2) = \frac{i\pi}{K^3} \begin{pmatrix} E_{12} k_2 k_1^2 \\ E_{12} k_1 k_2^2 \\ (E_{13} k_1 + E_{23} k_2) K^2 \end{pmatrix}. \tag{B 4}$$

Appendix C

In this appendix, we calculate the second term of the regular perturbation series, which comprises part of the solution to (2.7). This gives an $O(R_p B)$ correction to the Stokesian series. The matched asymptotic expansion presented in §3 is based upon $R_p/\alpha \ll 1$ and we show in §3.3 that for first-order matching, in most limits, it is unnecessary to calculate this regular perturbation expansion. However, we present the details of this calculation to confirm the matching approach of §3.3 and as it is required for second-order matching.

We pose expansion series for the non-dimensional disturbance velocity and pressure fields in the inner region as

$$w = w_0 + \frac{R_p}{\alpha} w_1 + \dots, \quad p = p_0 + \frac{R_p}{\alpha} p_1 + \dots, \tag{C 1}$$

The solution for w_0, p_0 is presented in §3.1 and the governing equations and boundary conditions for w_1 and p_1 are then given by

$$\nabla^2 w_1 - \nabla p_1 = w_0 \cdot \nabla w_0 + \bar{u}^* \cdot \nabla w_0 + w_0 \cdot \nabla \bar{u}^* - U_p^* \cdot \nabla w_0, \tag{C 2a}$$

$$\nabla \cdot w_1 = 0, \tag{C 2b}$$

$$w_1 = 0, \quad |x| = 1, \qquad w_1 \to 0, \quad |x| \to \infty. \tag{C 2c, d}$$

We consider this system of equations (C 2) as a creeping-flow problem with a forcing denoted by $Q = w_0 \cdot \nabla w_0 + \bar{u}^* \cdot \nabla w_0 + w_0 \cdot \nabla \bar{u}^* - U_p^* \cdot \nabla w_0$ and follow the approach of Saffman (1965) to derive an expression for the force exerted on the sphere at this order. If we denote

$$\int_{r=R} Q \, dS = \sum_n a_n R^n \quad \text{and} \quad \int_{r=R} x \nabla \cdot Q \, dS = \sum_n b_n R^n,$$

then the expression for the force is

$$F^{(1)} = \sum \frac{3}{2n} a_n + \sum \frac{(n-3)}{2n(n-2)} b_n + \tfrac{3}{2} C + \tfrac{1}{4} B - \frac{1}{2} \int_{r=R=1} x \frac{x \cdot Q}{R} \, dS, \tag{C 3}$$

where C, B are constants arising from the solution of the homogeneous part of (C 2). As demonstrated by Saffman (1965), these constants are important for asymptotic matching as C represents a uniform stream velocity and B is associated with a uniform pressure gradient and the resulting parabolic velocity profile.

The evaluation of the coefficients $\{a_n, b_n\}$ involves lengthy algebra, some of which is eased by the application of the following result:

$$\int_{r=R} \nabla_i \phi \, dS = \frac{d}{dR} \int_0^R \int_{r=constant} \nabla_i \phi \, dS \, dr \equiv \frac{d}{dR} \int_{1 \leqslant r \leqslant R} \nabla_i \phi \, dV,$$

$$= \frac{d}{dR} \int_{r=R} \phi n_i \, dS \quad \text{by the divergence theorem,}$$

$$= \frac{d}{dR} \int_{r=R} \frac{\phi x_i}{R} \, dS. \tag{C 4}$$

Applying this result, we find that

$$\int_{r=R} w_{0j} \nabla_j w_{0i} \, dS = \frac{d}{dR} \int_{r=R} \frac{w_{0j} w_{0i} x_j}{R} \, dS, \tag{C 5}$$

$$\int_{r=R} x_i \nabla_j (w_{0k} \nabla_k w_{0j}) \, dS = \frac{d}{dR} \left(\frac{1}{R} \frac{d}{dR} \int_{r=R} \frac{x_i x_j x_k w_{0k} w_{0j}}{R} \, dS \right)$$

$$- 2 \frac{d}{dR} \int_{r=R} \frac{x_j w_{0j} w_{0i}}{R} \, dS - \frac{d}{dR} \int_{r=R} \frac{x_i w_{0j} w_{0j}}{R} \, dS. \tag{C 6}$$

We may now substitute expressions for the velocity field in terms of Lamb's spherical harmonics, given by

$$\boldsymbol{w}_0 = \sum_n \nabla \psi_n + \boldsymbol{x} \wedge \nabla \chi_n + \frac{(n+3) \, r^2 \nabla p_n - 2nx p_n}{2(2n+3)(n+1)}. \tag{C 7}$$

We also note that for any harmonic function $f_n(\boldsymbol{x})$, $\boldsymbol{x} \cdot \nabla f_n = r(\partial/\partial r) f_n = n f_n$ and so

$$x_i w_{0i} = \sum_n n \psi_n + \frac{nr^2}{2(2n+3)} p_n. \tag{C 8}$$

For the problem under consideration here, Appendix A lists those spherical harmonics appropriate to the boundary condition $\boldsymbol{w} = 4\alpha^2 z^2 \hat{\boldsymbol{x}}$ on $r = 1$. The other harmonics we have are,

$$\psi_{-2} = \frac{U_p^* \cdot \boldsymbol{x}}{4r^3}, \quad p_{-2} = \frac{3}{2} \frac{U_p^* \cdot \boldsymbol{x}}{r^3}, \quad \psi_{-3} = -\frac{\boldsymbol{x} \cdot \boldsymbol{E} \cdot \boldsymbol{x}}{2r^5}, \quad p_{-3} = -5 \frac{\boldsymbol{x} \cdot \boldsymbol{E} \cdot \boldsymbol{x}}{r^5}. \tag{C 9}$$

With these expressions for the spherical harmonics appropriate to the problem under consideration, it is possible to evaluate integrals of the form (C 5), (C 6). For simplicity, we ignore the integrals involving the harmonics of $O(\alpha^2)$ as they yield corrections of $O(\alpha^2 R_p)$, which are certainly smaller than any of the corrections arising from the matched-asymptotic expansion analysis. However, in certain limits, the corrections of $O(BR_p)$ and $O(\alpha R_p)$, which arise from using the spherical harmonic components of the velocity field (C 9), are larger than the terms arising from the asymptotic matching.

To summarize the calculation then, we find the following:

$$\int_{r=R} w_{0j} \nabla_j w_{0i} \, dS = \pi E_{ij} U_{pj}^* \left(\frac{3}{R^2} - \frac{34}{5R^4} + \frac{3}{R^6} \right), \tag{C 10a}$$

$$\int_{r=R} x_i \nabla_j (w_{0k} \nabla_k w_{0j}) \, dS = \pi E_{ij} U_{pj}^* \left(-\frac{12}{R^2} + \frac{162}{5R^4} - \frac{24}{R^6} \right), \tag{C 10b}$$

$$\int_{r=R} w_{0j} \nabla_j \bar{u}_i \, dS = 4\pi E_{ij} U_{pj}^* R + 4\pi \epsilon_{ijk} \omega_j U_{pk}^* R, \tag{C 10c}$$

$$\int_{r=R} x_i \nabla_j (w_{0k} \nabla_k \bar{u}_j) \, dS = -\tfrac{6}{5} \pi E_{ij} U_{pj}^* R - 2\pi \epsilon_{ijk} \omega_j U_{pk}^* R, \tag{C 10d}$$

$$\int_{r=R} \bar{u}_j \nabla_j w_{0i} \, dS = \tfrac{4}{5} \pi E_{ij} U_{pj}^* R, \tag{C 10e}$$

$$\int_{r=R} x_i \nabla_j (\bar{u}_k \nabla_k w_{0j}) \, dS = -\tfrac{6}{5} \pi E_{ij} U_{pj}^* R - 2\pi \epsilon_{ijk} \omega_j U_{pk}^* R. \tag{C 10f}$$

So combining these integrals, we find that,

$$\int_{r=R} \boldsymbol{Q} \, \mathrm{d}S = \pi \boldsymbol{E} \cdot \boldsymbol{U}_p^* \left(\frac{24R}{5} + \frac{3}{R^2} - \frac{34}{5R^4} + \frac{3}{R^6} \right) + 4\pi \omega \wedge \boldsymbol{U}_p^* R, \tag{C 11}$$

$$\int_{r=R} x \boldsymbol{\nabla} \cdot \boldsymbol{Q} \, \mathrm{d}S = \pi \boldsymbol{E} \cdot \boldsymbol{U}_p^* \left(-\frac{12R}{5} - \frac{12}{R^2} + \frac{162}{5R^4} - \frac{24}{R^6} \right) - 4\pi \omega \wedge \boldsymbol{U}_p^* R. \tag{C 12}$$

Hence
$$\sum \frac{3}{2n} a_n = \tfrac{27}{4} \pi \boldsymbol{E} \cdot \boldsymbol{U}_p^* + 6\pi \omega \wedge \boldsymbol{U}_p^*, \tag{C 13}$$

$$\sum \frac{n-3}{2n(n-2)} b_n = -3\pi \boldsymbol{E} \cdot \boldsymbol{U}_p^* - 4\pi \omega \wedge \boldsymbol{U}_p^*. \tag{C 14}$$

Further
$$\int_{r=R} x \frac{x \cdot \boldsymbol{Q}}{R} \, \mathrm{d}S = \pi \boldsymbol{E} \cdot \boldsymbol{U}_p^* \left(\frac{8R^2}{5} + \frac{16}{15} + \frac{3}{R} - \frac{128}{15R^3} + \frac{21}{5R^5} \right) + \pi \boldsymbol{U}_p^* \wedge \omega(-1 + R^2),$$

$$= \tfrac{4}{3} \pi \boldsymbol{E} \cdot \boldsymbol{U}_p^* \quad \text{when} \quad R = 1. \tag{C 15}$$

Therefore combining these results, we find that

$$\boldsymbol{F}^{(1)} = \tfrac{37}{12} \pi \boldsymbol{E} \cdot \boldsymbol{U}_p^* + 2\pi \omega \wedge \boldsymbol{U}_p^*. \tag{C 16}$$

This first-order regular perturbation correction to the velocity is of $O(BR_p)$ and we note there is no term of $O(\alpha R_p)$. We also note that the regular perturbation correction involves terms like $\boldsymbol{E} \cdot \boldsymbol{U}_p^*$, $\omega \wedge \boldsymbol{U}_p^*$, which have no lateral component, if $\boldsymbol{U}_p^* = U_p \hat{z}$. Hence, in this case, they cannot be matched to the lateral component of the outer correction to the velocity field.

Appendix D

In this appendix, we consider the coupled differential equations for the transformed velocity and pressure fields in the limit of large Fourier mode number and find the asymptotic form of the velocity field at the origin. We have a no-slip boundary condition on the channel boundaries and consider the pressure-field jump conditions at the origin, relevant to §§4.1 and 4.2. So writing $k_1 = K \cos \theta$ and $k_2 = K \sin \theta$, equations (4.4) and no-slip boundary condition are

$$\frac{\mathrm{d}^2 \tilde{P}}{\mathrm{d}Z^2} - K^2 \tilde{P} = -2iK \cos \theta \tilde{W} (\gamma \alpha - 8\alpha^2 Z / R_c^{\frac{1}{2}}), \tag{D 1}$$

$$\frac{\mathrm{d}^2 \tilde{W}}{\mathrm{d}Z^2} - K^2 \tilde{W} = \frac{\mathrm{d}\tilde{P}}{\mathrm{d}Z} + iK \cos \theta \tilde{W} (\gamma \alpha Z - 4\alpha^2 Z^2 / R_c^{\frac{1}{2}}), \tag{D 2}$$

$$\tilde{W} = \frac{\mathrm{d}\tilde{W}}{\mathrm{d}Z} = 0, \quad Z = Z^+, Z^-; \quad Z^+ - Z^- = R_c^{\frac{1}{2}}. \tag{D 3}$$

We analyse this system of equations in the limit $K \to \infty$. We introduce $\epsilon = 1/K$ and seek an asymptotic expression for $\tilde{W}$ in the regime $0 < \epsilon \ll 1$. Equations (D 1) and (D 2) admit two asymptotic regions; $Z = O(1)$, $Z = O(\epsilon)$. If $Z^+, Z^- \sim O(1)$ then both boundaries lie in the 'outer' region ($Z = O(1)$). Hence, applying the no-slip boundary condition (D 3), we find that the outer velocity and pressure fields vanish at all algebraic orders. Thus we are forced to select the exponentially decaying solutions

within the inner region. If, however, $Z^+ = O(\epsilon)$ (or $Z^- = O(\epsilon)$), then one of the boundaries falls within the 'inner' region ($Z = O(\epsilon)$). This means that while on one side of the origin we may take the decaying solution, on the other we are forced to include both the decaying and growing exponentials. We introduce a rescaled variable $\eta = Z/\epsilon$ and denote $\mathscr{P}(\eta) = \tilde{P}(Z)$, $\mathscr{W}(\eta) = \tilde{W}(Z)$. The equations to be solved are then

$$\frac{\mathrm{d}^2\mathscr{P}}{\mathrm{d}\eta^2} - \mathscr{P} = -2\mathrm{i}\epsilon\cos\theta\mathscr{W}\left(\gamma - \frac{8\epsilon\eta}{R_c^{\frac{1}{2}}}\right), \tag{D 4}$$

$$\frac{\mathrm{d}^2\mathscr{W}}{\mathrm{d}\eta^2} - \mathscr{W} = \epsilon\frac{\mathrm{d}\mathscr{P}}{\mathrm{d}\eta} + \mathrm{i}\epsilon\left(\gamma\epsilon\eta - \frac{4\epsilon^2\eta^2}{R_c^{\frac{1}{2}}}\right)\cos\theta\mathscr{W}. \tag{D 5}$$

We propose the following series expansions:

$$\mathscr{P} = \mathscr{P}_0 + \epsilon\mathscr{P}_1 + \epsilon^2\mathscr{P}_2 + O(\epsilon^3), \quad \mathscr{W} = \mathscr{W}_0 + \epsilon\mathscr{W}_1 + \epsilon^2\mathscr{W}_2 + O(\epsilon^3).$$

If $Z^+, Z^- \sim O(1)$ then we solve (D 4) and (D 5) by finding the appropriate decaying solutions which satisfy the prescribed jump conditions at the origin. If, however, $Z^+ = O(\epsilon)$ then we must enforce the boundary condition at $\eta^+ = Z^+/\epsilon$. We find that the boundaries lead to contributions of $O(\exp(-2\eta^+))$ and so are only significant when $\eta^+ = O(1)$. We present the asymptotic analysis for both the horizontally and vertically aligned channels.

D.1. *Horizontally aligned channel*

The jump condition is on the pressure field at the origin,

$$[\tilde{P}]_{Z=0^-}^{Z=0^+} = [\mathscr{P}]_{\eta=0^-}^{\eta=0^+} = \frac{3}{2\pi}. \tag{D 6}$$

Hence, we find that the transform velocity field at the origin is

$$\mathscr{W}(\eta = 0) = \frac{3\epsilon}{8\pi} - \frac{3\mathrm{i}\gamma\cos\theta\epsilon^3}{32\pi} - \frac{3\epsilon}{8\pi}\exp(-2\eta^+)(2\eta^{+2} + 2\eta^+ + 1) + O(\mathrm{i}\epsilon^4). \tag{D 7}$$

Hence the large Fourier mode number component of the inversion integral (5.9) may be evaluated as follows:

$$\mathrm{Re}\left\{\int_0^{2\pi}\int_{K_m}^{\infty}\left(\tilde{W}(Z=0) - \frac{3}{8\pi K}\right)K\,\mathrm{d}K\,\mathrm{d}\theta\right\}$$

$$= -\frac{3}{4Z^+}\exp(-2K_m Z^+)((K_m Z^+)^2 + 2K_m Z^+ + \tfrac{3}{2}) + O(K_m^{-1}). \tag{D 8}$$

D.2. *Vertically aligned channel*

The jump condition is on the derivative of the pressure field at the origin,

$$\left[\frac{\mathrm{d}\tilde{P}}{\mathrm{d}Z}\right]_{Z=0^-}^{Z=0^+} = \left[\frac{1}{\epsilon}\frac{\mathrm{d}\mathscr{P}}{\mathrm{d}Z}\right]_{\eta=0^-}^{\eta=0^+} = \frac{\mathrm{i}3K\cos\theta}{2\pi\epsilon}. \tag{D 9}$$

Hence, we find that the transform velocity field at the origin is

$$\mathscr{W}(\eta = 0) = -\frac{3\gamma\cos^2\theta\epsilon^3}{16\pi} - \frac{3\gamma\cos^2\theta\epsilon^3}{16\pi}$$

$$\times \exp(-2\eta^+)(-\tfrac{1}{3}\eta^{+4} + \tfrac{1}{3}\eta^{+3} - \tfrac{8}{3}\eta^{+2} - \tfrac{5}{3}\eta^+ - 1) + O(\epsilon^5). \tag{D 10}$$

Hence the large Fourier mode number component of the inversion integral (5.9) may be evaluated as follows:

$$\mathrm{Re}\left\{\int_0^{2\pi}\int_{K_m}^{\infty}\tilde{W}(Z=0)\,K\,\mathrm{d}K\,\mathrm{d}\theta\right\}=-\frac{3\gamma}{16K_m}-\frac{3\gamma Z^+}{16}(\exp\,(-2K_m z^+)\,(-\tfrac{1}{6}(K_m z^+)^2$$

$$+\tfrac{1}{12}K_m z^+ +\tfrac{11}{8})+\tfrac{5}{3}E_1(2K_m Z^+)-2E_2(2K_m Z^+)) \quad \text{(D 11)}$$

where
$$E_j(X)=\int_X^{\infty}\frac{\exp\,(-Y)}{Y^j}\,\mathrm{d}Y.$$

Appendix E. The lift on a sphere in unbounded linear shear flow

In this appendix we study the motion of a small particle with an arbitrary directed velocity, moving within an unbounded linear shear flow. This calculation was first made by Saffman (1965), to study the lift on a spherical particle moving parallel with the undisturbed flow. Subsequently, Harper & Chang (1968) generalized the calculation to permit the particle to have an arbitrary directed velocity. This appendix demonstrates how Harper & Chang's result may be derived from the analysis presented in the main body of this paper. It also shows how the study of McLaughlin (1991) fits in with this and previous work. Therefore, we include few details of the calculation as they have been published before, but we clarify whether the inertial drag or lift force on the particle changes direction with reversing the sign of the shear coefficient of the undisturbed flow. This issue is not made explicit by the previous studies.

We consider an undisturbed linear shear flow, denoted by $\bar{u}=\Gamma z\hat{x}$, where $\Gamma \geqslant 0$. Hence we have the following non-dimensional parameters to characterize the problem: the particle Reynolds number, $\mathcal{R}=|\Gamma|a^2/\nu$ and the buoyancy number $B=\tfrac{2}{9}a\Delta\rho g/\mu|\Gamma|$. Then if we non-dimensionalize velocities with respect to $|\Gamma|a$ and lengths with respect to a, the governing equations and boundary conditions for the disturbance flow are

$$\mathcal{R}\left(\frac{\partial w}{\partial t}+w\cdot\nabla w+\bar{u}^*\cdot\nabla w-U_p^*\cdot\nabla w+w\cdot\nabla\bar{u}^*\right)=-\nabla p+\nabla^2 w, \qquad \text{(E 1}a\text{)}$$

$$\nabla\cdot w=0, \qquad \text{(E 1}b\text{)}$$

$$w=U_p^*+\Omega\wedge x-\bar{u}^*, \quad |x|=1, \qquad w\to 0, \quad |x|\to\infty, \qquad \text{(E 1}c,d\text{)}$$

$$\int_{|x|=1}\sigma(w)\cdot\hat{n}\,\mathrm{d}S=-6\pi B\hat{g}, \qquad \text{(E 1}e\text{)}$$

where the undisturbed flow with respect to this new origin is given by $\bar{u}^*=\mathrm{sgn}\,(\Gamma)z\hat{x}$.

These equations are solved by means of matched asymptotic expansions, under the assumption that the particle Reynolds number is small compared to unity. We construct inner and outer regions: the inner region is Stokesian, dominated by viscous forces, whereas the outer region exhibits a balance between viscous and inertial forces. The inner problem is solved in an identical manner to §3.1, with the simplification that there is no $O(\alpha^2)$ term. Furthermore, the far-field is dominated by the Stokeslet contribution as this decays like $O(1/r)$, whereas the velocity field resulting from the shear decays like $O(1/r^2)$. This implies that there is only one matching possibility and it takes the form of a delta-function forcing in the momentum equation (see §3.3).

In the outer region, we find that there are two scaling possibilities:
(i) viscous terms balance inertial advective terms due to undisturbed shear velocity,

$$S=\mathcal{R}^{\frac{1}{2}} \quad \text{if} \quad 1\gg\mathcal{R}B^2;$$

(ii) viscous terms balance inertial advective terms due to sphere migration

$$S = \mathcal{R}B \quad \text{if} \quad 1 \ll \mathcal{R}B^2.$$

Case (ii) is the appropriate limit for a heavy sphere, moving through weak background flow. This recovers the governing equations proposed by Oseen for a sphere translating through quiescent fluid. Case (i) is the scaling for the problem studied by Saffman (1965) and Harper & Chang (1968). The intermediate regime $\mathcal{R}B^2 \sim O(1)$ was studied by McLaughlin (1991) and he presented both numerical and asymptotic analysis of the problem.

To complete this discussion of the small inertial effects in unbounded linear shear flow, we focus on the regime $\mathcal{R}B^2 \ll 1$ and recover equations similar to those studied by Harper & Chang (1968). As in §3.3, we denote the velocity and pressure fields in the outer region by $P(X) = p(x)$, $W(X) = w(x)$ and we pose expansion series

$$W(X) = W_0(X) + \dots, \quad P(X) = SP_0(X) + \dots.$$

Thus, we have the following system of equations

$$\nabla^2 W_0 - \nabla P_0 = \text{sgn}\,(\Gamma)\, Z \frac{\partial W_0}{\partial X} + \text{sgn}\,(\Gamma)\, W_0 \cdot \hat{Z}\hat{X}, \tag{E 3a}$$

$$\nabla \cdot W_0 = 0, \tag{E 3b}$$

$$W_0 \to 0, \quad |X| \to \infty, \tag{E 3c}$$

$$W_0 \sim \left(U_p^* \frac{3}{4R} + x \frac{U_p^* \cdot x}{R^2} \frac{3}{4R} \right) S, \quad X \sim 0. \tag{E 3d}$$

We take three-dimensional Fourier transforms of these equations and consider

$$W_{migration} = \lim_{R \to 0} \left(W_0(X) - S \left(U_p^* \frac{3}{4R} + x \frac{U_p^* \cdot x}{R^2} \frac{3}{4R} \right) \right). \tag{E 4}$$

Hence we find that

$$W_{migration\,i} = \mathcal{R}^{\frac{1}{2}} \Lambda_{ij}\, U_{pj}, \tag{E 5}$$

where

$$\Lambda_{ij} = \begin{pmatrix} 0.944 & 0 & \text{sgn}\,(\Gamma)\,0.620 \\ 0 & 0.703 & 0 \\ \text{sgn}\,(\Gamma)\,0.343 & 0 & 0.326 \end{pmatrix}.$$

In the derivation of this result, we assume that there is a small particle Reynolds number ($\mathcal{R} \ll 1$), the shear flow is dominant ($\mathcal{R}B^2 \ll 1$) and the particle Reynolds number based on rotation is small ($\Omega_p a^2 / \nu \ll 1$). The second of these conditions may alternatively be expressed as the ratio of the square of the particle Reynolds number based on slip velocity to the particle Reynolds number based on shear rate ($\mathcal{R}B^2 = R_{U_p}^2 / \mathcal{R}$), which corresponds to the expression of this ratio used by previous studies (Saffman 1965; Harper & Chang 1968).

REFERENCES

ABBOTT, J. E. & FRANCIS, J. R. D. 1977 Saltation and suspension trajectories of solid grains in a water stream. *Phil. Trans. R. Soc. Lond.* A **284**, 225–254.

BATCHELOR, G. K. 1965 *An Introduction to Fluid Dynamics*. Cambridge University Press.

BRENNER, H. 1961 The slow motion of a sphere through a viscous fluid towards a plane surface. *Chem. Engng Sci.* **16**, 242–251.

BRETHERTON, F. P. 1962 The motion of rigid particles in a shear flow at low Reynolds number. *J. Fluid Mech.* **14**, 284–304.

BROUSSE, R. 1965 Observations sur les dykes et leur prismation. *Congrès des Sociétés Sauvant, Nice.*

COX, R. G. & HSU, S. K. 1977 The lateral migration of solid particles in a laminar flow near a plane. *Intl. J. Multiphase Flow* **3**, 201–222.

DREW, D. A. 1978 The force on a small sphere in slow viscous flow. *J. Fluid Mech.* **88**, 393–400.

DREW, D. A. 1988 The lift force on a small sphere in the presence of a wall. *Chem. Engng Sci.* **43**, 769–773.

EICHHORN, R. & SMALL, S. 1964 Experiments on the lift and drag of spheres suspended in a Poiseuille flow. *J. Fluid Mech.* **20**, 513–527.

GANATOS, P., WEINBAUM, S. & PFEFFER, R. 1980 A strong interaction theory for the creeping motion of a sphere between parallel boundaries. Part 1: Perpendicular motion. *J. Fluid Mech.* **99**, 739–753.

GIDDINGS, J. C., MYERS, M. N., MOON, M. H. & BARMAN, B. N. 1991 Particle separation and size characterisation by sedimentation field-flow fractionation. *Particle-Size Distribution II.* ACS Symposium Series 472, Provder.

HAPPEL, J. & BRENNER, H. 1965 *Low Reynolds Number Hydrodynamics.* Prentice-Hall.

HARPER, E. Y. & CHANG, I.-D. 1968 Maximum dissipation resulting from lift in slow viscous flow. *J. Fluid Mech.* **33**, 209–225.

HINCH, E. J. 1992 *Perturbation Methods.* Cambridge University Press.

HO, B. P. & LEAL, L. G. 1974 Inertial migration of rigid spheres in two dimensional unidirectional flows. *J. Fluid Mech.* **65**, 365–400.

JEFFREY, R. C. & PEARSON, J. R. A. 1965 Particle motion in laminar vertical tube flow. *J. Fluid Mech.* **22**, 721–735.

LAMB, H. 1932 *Hydrodynamics.* Cambridge University Press.

LIN, C.-J., PERRY, J. H. & SCHOWALTER, W. R. 1970 Simple shear flow round a rigid sphere: inertial effects and suspension rheology. *J. Fluid Mech.* **44**, 1–17.

LISTER, J. R. & KERR, R. C. 1991 Fluid-mechanical models of crack propagation and their application to magma transport in dykes. *J. Geophys. Res.* **96B**, 10049–10077.

MCLAUGHLIN, J. B. 1991 Inertial migration of a small sphere in linear shear flows. *J. Fluid Mech.* **224**, 261–274.

MCLAUGHLIN, J. B. 1993 The lift on a small sphere in wall-bounded linear shear flows. *J. Fluid Mech.* **246**, 249–265.

SAFFMAN, P. G. 1965 The lift on a small sphere in slow shear flow. *J. Fluid Mech.* **22**, 385–400, and Corrigendum *J. Fluid Mech.* **31**, 1968, 624.

SCHONBERG, J. A. & HINCH, E. J. 1989 Inertial migration of a sphere in Poiseuille flow. *J. Fluid Mech.* **203**, 517–524.

SEGRÉ, G. & SILBERBERG, A. 1962a Behaviour of macroscopic rigid spheres in Poiseuille flow. Part 1. Determination of local concentration by statistical analysis of particle passages through crossed light beams. *J. Fluid Mech.* **14**, 115–135.

SEGRÉ, G. & SILBERBERG, A. 1962b Behaviour of macroscopic rigid spheres in Poiseuille flow. Part 2. Experimental results and interpretation. *J. Fluid Mech.* **14**, 136–157.

SHIBATA, M. & MEI, C. C. 1990 Inertia effects of a localised force distribution near a wall in a slow shear flow. *Phys. Fluids* A **2**, 1094–1104.

VASSEUR, P. & COX, R. G. 1976 The lateral migration of a spherical particle in two dimensional shear flows. *J. Fluid Mech.* **78**, 385–413.

VASSEUR, P. & COX, R. G. 1977 The lateral motion of spherical particles sedimenting in a stagnant bounded fluid. *J. Fluid Mech.* **80**, 561–591.